Trace element geochemistry of the 1991 Mt. Pinatubo silicic melts, Philippines: Implications for ore-forming potential of adakitic magmatism.

Anastassia Yu Borisova, Michel Pichavant, Mireille Polvé, Michael Wiedenbeck, Rémi Freydier, Frédéric Candaudap

Trace element geochemistry of the 1991 Mt. Pinatubo silicic melts, Philippines: Implications for ore-forming potential of adakitic magmatism

Anastassia Yu. Borisova[a, b], Michel Pichavant[c], Mireille Polvé[a], Michael Wiedenbeck[d], Remi Freydier[a] and Frédéric Candaudap[a]

[a]Laboratoire des Mécanismes et Transferts en Géologie, LMTG – UMR 5563 – OMP – CNRS, 14 Avenue E. Belin, 31400 Toulouse, France
[b]Vernadsky Institutes of Geochemistry and Analytical Chemistry, RAS Kosiguin str., 19, 117975 Moscow, Russia
[c]Institut des Sciences de la Terre d'Orléans, CNRS-ISTO, 1A, rue de la Férollerie 45071 Orléans, Cedex 2, France
[d]GeoForschungsZentrum Potsdam, Telegrafenberg, D14473 Potsdam, Germany

Abstract

The dacite pumice erupted from Mt. Pinatubo on June 15, 1991 (whole-rock, rhyolitic groundmass glasses and homogenized melt inclusions) has been analyzed using inductively coupled plasma-mass spectrometry (ICP-MS), nanosecond and femtosecond laser ablation ICP-MS and secondary ion mass spectrometry (SIMS) to evaluate its ore-forming potential. Data suggest that adakite magmas are metal-rich and concentrate ore metals during magmatic differentiation. Sulfides segregate in limited amounts under the hydrous, oxidizing conditions typical of adakitic magmas resulting in incompatible behavior for Au (6–22 ppb), Cu (26–77 ppm), and Pb, Mo, As, and Sb in melts of dacitic to rhyolitic compositions. Metal transfer from this adakite magma to the coexisting aqueous phase was favored by the peraluminous composition of the rhyolitic melt and high aqueous chloride concentrations. Mass balance calculations suggest that the pre-eruptive aqueous phase could have extracted a minimum of 100 t Au and 5×10^5 t Cu from the Mt. Pinatubo magma. Our data suggest that intrusives having adakitic signatures are genetically associated with Au–Cu and Cu–Mo mineralization, auriferous porphyry copper deposits, and epithermal gold veins. High H_2O, Cl, Sr/Y, Pb/Ce, Mo/Ce, As/Ce and Sb/Ce in Mt. Pinatubo melts reflect the contribution of deep fluids derived from subducted sediments and altered MORBs in the dacite genesis. The slab-derived fluids carrying mobile elements are likely responsible for the enrichment of adakite magmas in gold, associated metals and H_2O, and may explain the exceptional ore-forming potential of adakite magmatism.

1. Introduction

Adakites are silicic- to intermediate-composition magmas which are commonly believed to be generated by partial melting of subducted oceanic crust (e.g., Defant and Drummond, 1990 and Sen and Dunn, 1994), although other models, such as high-pressure fractionation of hydrous basaltic magmas, have also been proposed recently for their genesis (e.g., Prouteau and Scaillet, 2003). Adakitic magmas are typically enriched in H_2O (Prouteau et al., 1999) and lithophile elements such as Al, Na, Sr and LREE (Drummond and Defant, 1990 and Peacock et al., 1994). Intrusives with an adakitic signature are spatially and temporally and, perhaps, genetically associated with Au–Cu and Cu–Mo mineralization, auriferous porphyry

copper deposits, and epithermal gold veins (e.g., White et al., 1995, Sajona and Maury, 1998, González-Partida et al., 2003, Reich et al., 2003, Qu et al., 2004 and Whalen et al., 2004). However, the petrological and geochemical mechanisms which are responsible for the systematic relationship between adakitic magmatic rocks and gold and associated metals concentrations remain unclear (Thiéblemont et al., 1997 and Mungall, 2002). Understanding the mechanisms that control the links between adakitic magmas and Au–Cu (and Cu–Mo) mineralization is important both for metallogenic models and associated metals exploration strategies.

In this study, we assume as a working hypothesis that adakite magmas are enriched in Au (typically 3–7 ppb) in comparison with non-adakitic (typically <3 ppb), silicic- to intermediate-composition magmas (Polvé et al., 2003, Polvé et al., 2004 and Jégo et al., 2004). Thus, adakites are able to pre-concentrate Au (with Cu and associated metals) through magmatic processes. The systematic association between adakites and Au–Cu mineralization (e.g., Thiéblemont et al., 1997) would thus result from the combination of magmatic pre-concentration mechanisms with favorable hydrothermal transport and deposition processes. To investigate the magmatic pre-concentration mechanisms, we have carried out an analytical study of a typical example of adakite, the dacite pumice erupted on June 15, 1991, by the Mt. Pinatubo volcano, Philippines (Bernard et al., 1996, Prouteau et al., 1999 and Prouteau and Scaillet, 2003).

The Mt. Pinatubo dacite is strongly enriched in sulfur (e.g., Bernard et al., 1996), Cu and Zn (Pallister et al., 1996). The $\delta^{34}S$ values for the 1991 dacite are similar to those of Cu–Au porphyry deposits of Miocene to Pliocene ages surrounding Mt. Pinatubo (Imai et al., 1993 and Imai et al., 1996). Located south of the North Luzon Au–Cu province of Miocene–Pliocene age, Mt. Pinatubo is only 19 km north of the 2.7 Ma Dizon major Cu–Au porhyry copper deposit (Malihan, 1987), and several porphyry-type prospects are known in its immediate vicinity (Imai et al., 1996; Fig. 1). Therefore, metal concentration processes in the 1991 Mt. Pinatubo magma may be representative of those occurring in the North to West-Central Luzon Au–Cu district.

The Mt. Pinatubo dacite preserves rapidly quenched silicate glasses and sulfides, allowing metal concentrations to be determined at different stages of the magmatic evolution. Previous work on melt, crystal and fluid inclusions in mineral phases of the Mt. Pinatubo white dacite pumices (Westrich and Gerlach, 1992, Gerlach et al., 1996, Pasteris et al., 1996, Rutherford and Devine, 1996 and Borisova et al., 2005), together with experimental data (Rutherford and Devine, 1996, Scaillet and Evans, 1999, Prouteau et al., 1999 and Prouteau and Scaillet, 2003) have constrained the conditions of genesis, high-pressure evolution, and pre-eruptive crystallization and degassing of the dacite magma. The chalcophile trace element chemistry of sulfide phases in the Mt. Pinatubo dacites, andesites and basalts has been investigated by Fournelle et al., 1996, Hattori, 1993 and Hattori, 1996. However, there are as yet no data on ore metal concentrations for the silicate glasses. Here, we present an in situ microanalytical study of volatiles (H_2O) and ore metals (Cu, Zn, Mo and Pb) in homogenized melt inclusions using secondary ion mass spectrometry (SIMS). These data are combined with microanalyses of trace elements (including Au) in matrix glasses using nanosecond and femtosecond laser ablation ICP-MS, and with analyses of the host dacite pumice using ICP-MS. The data reported here constrain the trace element chemistry of the Mt. Pinatubo melts and provide new insights into mechanisms of metal pre-concentration during adakitic magma genesis and differentiation.

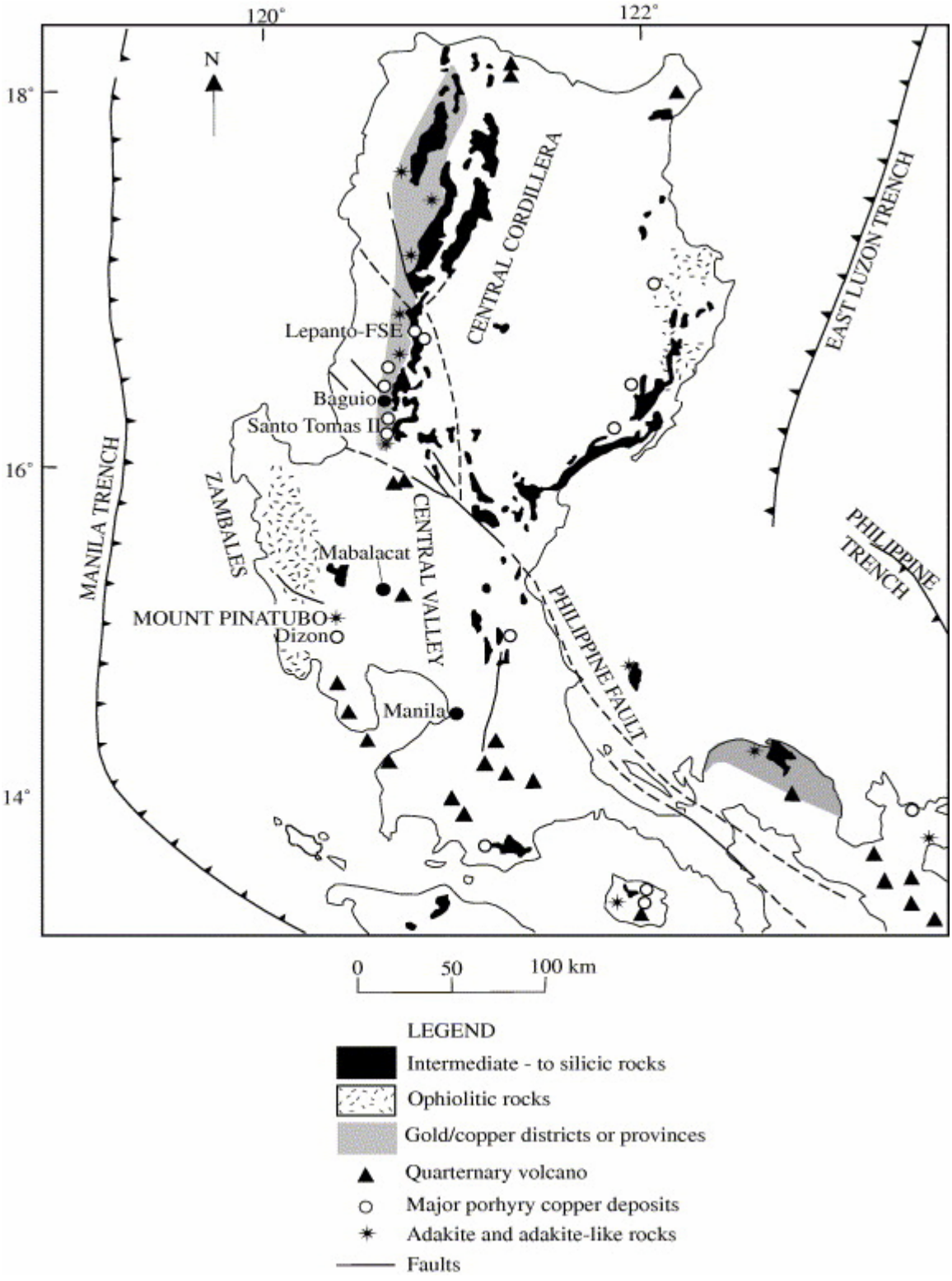

Fig. 1. Geologic map showing the location of quaternary volcanoes, major porphyry copper deposits, Cenozoic intermediate to silicic intrusives, and ophiolitic rocks at Luzon, Philippines (adopted after Imai et al., 1996 and modified after Sajona and Maury, 1998). Tertiary intermediate to felsic intrusives and ophiolitic rocks are also shown. Adakite and adakite-like rocks related to gold-copper districts or provinces are shown according to Sajona and Maury (1998).

The Mt. Pinatubo dacite preserves rapidly quenched silicate glasses and sulfides, allowing metal concentrations to be determined at different stages of the magmatic evolution. Previous work on melt, crystal and fluid inclusions in mineral phases of the Mt. Pinatubo white dacite pumices (Westrich and Gerlach, 1992, Gerlach et al., 1996, Pasteris et al., 1996, Rutherford and Devine, 1996 and Borisova et al., 2005), together with experimental data (Rutherford and Devine, 1996, Scaillet and Evans, 1999, Prouteau et al., 1999 and Prouteau and Scaillet, 2003) have constrained the conditions of genesis, high-pressure evolution, and pre-eruptive crystallization and degassing of the dacite magma. The chalcophile trace element chemistry of sulfide phases in the Mt. Pinatubo dacites, andesites and basalts has been investigated by Fournelle et al., 1996, Hattori, 1993 and Hattori, 1996. However, there are as yet no data on ore metal concentrations for the silicate glasses. Here, we present an in situ microanalytical study of volatiles (H_2O) and ore metals (Cu, Zn, Mo and Pb) in homogenized melt inclusions using secondary ion mass spectrometry (SIMS). These data are combined with microanalyses of trace elements (including Au) in matrix glasses using nanosecond and femtosecond laser ablation ICP-MS, and with analyses of the host dacite pumice using ICP-MS. The data reported here constrain the trace element chemistry of the Mt. Pinatubo melts and provide new insights into mechanisms of metal pre-concentration during adakitic magma genesis and differentiation.

2. Analytical techniques

2.1. Melt inclusion and matrix preparation for analyses

Primary melt inclusions in quartz were completely or partially homogenized at 760 °C and 200 MPa. Detailed descriptions of melt inclusion types before and after homogenization experiments and of the experimental procedures are given in Borisova et al. (2005) along with major element data on the included glass and crystalline phases. The experimental run duration of 20–24 h was chosen according to the diffusion rates of H_2O and CO_2 in silicic glasses (Watson, 1994) to produce homogeneous glasses in the melt inclusions. The melt inclusions range in size from 30 to 150 μm and contain homogeneous glasses; only inclusions with minor or no bubble(s) were selected (Fig. 2). After the homogenization experiment, quartz grains were mounted in epoxy (Teflon slides, 1-in. diameter) and polished by hand with 3-, 1- and 0.5-μm diamond pastes (Hyprez, Liquid Diamond) until the melt inclusions were exposed at the surface (Borisova et al., 2005). To avoid possible surface contamination with metals like Au, Cu, Zn, As and Sb, we polished quartz grains with pure diamond pastes. Thick sections (300 μm) of dacite pumices and <0.5-mm pieces of matrix glasses were epoxy-mounted and polished with precautions as well to avoid surface contamination with gold and base metals.

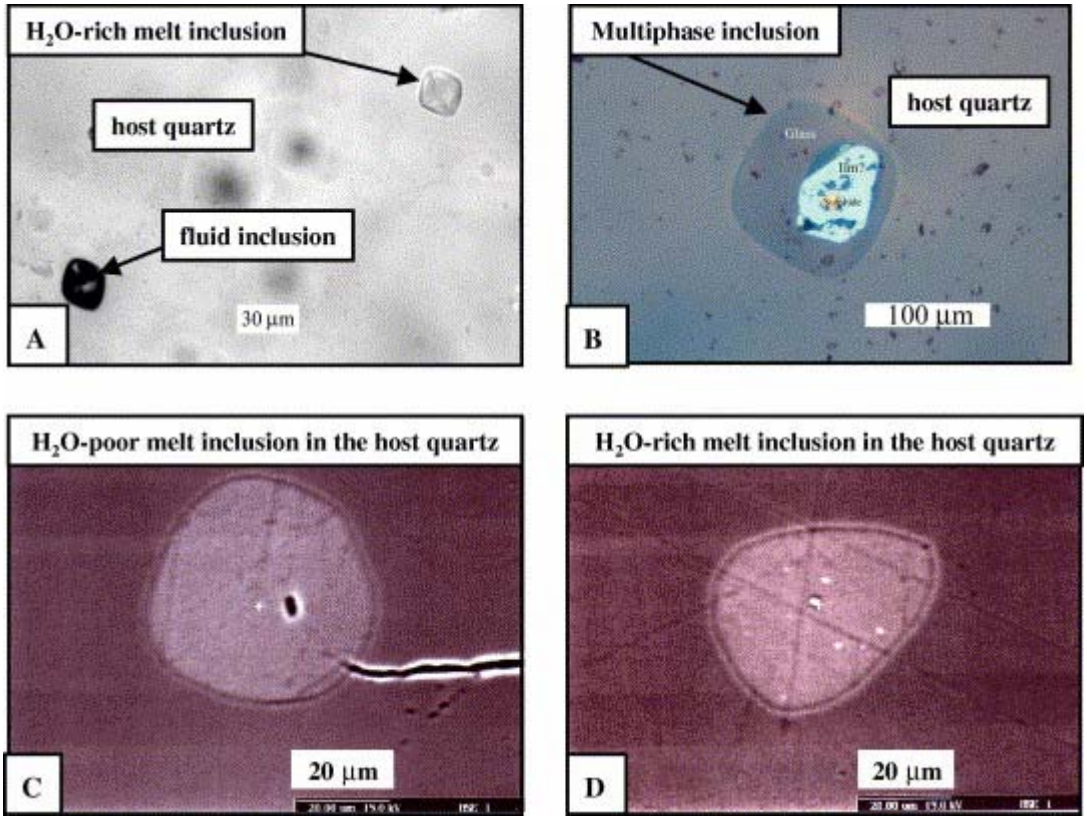

Fig. 2. Photomicrographs of inclusions after homogenization experiment: (A) Assemblage of primary fluid inclusion, at present empty (left) and primary melt inclusion (right) homogenized at 780 °C and 185 MPa, providing evidence for two-phase entrapment of coexisting melt and supercritical fluid under pre-eruptive conditions (in transmitted light); (B) Multi-phase inclusion after experiment at 780 °C and 185 MPa containing sulfide globule (center) entrapped in ilmenite and enclosed in rhyolitic melt (in reflected light); (C) Decrepitated (H_2O-poor) melt inclusion (in back-scattered electron mode); (D) Stable (H_2O-rich) melt inclusion homogenized at 760 °C and 200 MPa (in back-scattered electron mode).

2.2. Analytical techniques

Major elements concentrations in the inclusion glasses were determined by electron microprobe analysis (EMPA) with a fully automated CAMECA SX-100 in GeoForschungsZentrum in Potsdam, Germany. X-ray were excited with a 15-kV accelerating voltage and 10 nA beam current. The acquisition time for major elements (Si, Ti Al, Fe, Mg, Ca, Na and K) was 20 s/element. A defocused beam ($\sim$15 µm^2) was used to minimize Na loss. The following EMPA standards were used: albite (Na), periclase (Mg), wollastonite (Si, Ca), Fe_2O_3 (Fe), rutile (Ti) and orthoclase (Al, K). Groundmass glasses and sulphide analyses were performed at the Laboratoire des Mécanismes et Transferts en Géologie (Toulouse, France) using a CAMECA SX50 microprobe with SAMx automation. The operating conditions were 15 kV of accelerating voltage and 10 nA of beam current for glasses, and 25 kV of accelerating voltage and 20 nA of beam current for sulphides. Standards were synthetic compounds and natural minerals. Following electron microprobe analysis, the epoxy mounts were slightly polished with pure Al_2O_3 powder (0.3-µm) to remove the carbon coating, cleaned in ethanol (Normapur grade), dried at 80 °C for 1 h to remove surface water, and then gold coated for secondary ion mass spectrometric (SIMS) analyses.

SIMS analyses of H and selected trace elements Cu, Zn, Pb, Mo, La, Ce and Pr were performed using the CAMECA ims 6f ion probe in GeoForschungsZentrum, Potsdam. To

eliminate any possible surface contamination and to remove the 35-nm gold coat, each analysis spot was pre-sputtered for 3 min with a 12-nA $^{16}O^-$ beam which was rastered over a 25 × 25 μm area. The actual analyses recorded the intensities on the $^{1}H^+$, $^{30}Si^+$, $^{64}Zn^+$, $^{65}Cu^+$, $^{139}La^+$, $^{140}Ce^+$, $^{141}Pr^+$, $^{98}Mo^+$ and $^{208}Pb^+$ peaks using a primary beam intensity of 8 nA focused to a ~25-μm diameter spot on the sample surface. A 120-V offset was applied to the nominally 10 kV, in conjunction with a 50-V energy bandpass, in order to suppress isobaric interferences (e.g., Hervig, 1996). Counting times for each cycle were: $^{1}H^+$ (4 s), $^{30}Si^+$ (2 s), $^{44}Ca^+$ (2 s), $^{64}Zn^+$ (8 s), $^{65}Cu^+$(8 s), $^{98}Mo^+$ (30 s), $^{139}La^+$ (8 s), $^{140}Ce^+$(15 s), $^{141}Pr^+$ (15 s) and $^{208}Pb^+$ (30 s). Twenty integration cycles of this peak-stepping sequence thus yielded a total analysis time of 46 min. The host quartz grains were used to estimate the water background which was consistently below 0.1 wt% H_2O. The count rates from $^{1}H^+$, $^{64}Zn^+$, $^{65}Cu^+$, $^{98}Mo^+$, $^{139}La^+$, $^{140}Ce^+$, $^{141}Pr^+$ and $^{208}Pb^+$ were normalized to $^{30}Si^+$. The intensities of either $^{1}H/^{30}Si$, $^{64}Zn/^{30}Si$ or $^{65}Cu/^{30}Si$ signals in some glasses decayed and attained constant values only after the first 10 cycles of data collection; in this case only the data obtained in the last 5–10 cycles were used to calculate the element abundances (Table 1). The concentrations of water and trace elements in the glass samples were determined by SIMS using calibrations with reference glasses of known concentrations (see electronic annex, Table EA1). For H^+ a calibration curve was established from the nominally anhydrous NIST SRM 610 glass, a series of hydrated glasses prepared from NIST 610 and a series of hydrated andesitic glasses (see Wiedenbeck et al., 2001 and Koepke and Behrens, 2001). For the trace elements calibration we used anhydrous glasses, such as NIST SRM 610 glass, the above mentioned synthetic andesitic glass, and natural rhyolitic obsidian Macusani (or MAC3, electronic annex, Table EA1). All these reference samples were checked for homogeneity with respect to trace element contents by LA-ICP-MS, and trace element concentrations in Macusani glasses were re-analyzed by ICP-MS (electronic annex, Table EA1). Calibration curves were prepared by plotting the measured $M^+/^{30}Si^+$ ratios of standards against their trace element concentrations, normalizing to silicon concentrations (in ppm) known or obtained by EMPA (see electronic annex, Fig. EA1–EA8). We did not detect any dependence of the relative sensitivity factors of $^{65}Cu/^{30}Si$, $^{98}Mo/^{30}Si$, $^{139}La/^{30}Si$, $^{140}Ce/^{30}Si$ and $^{141}Pr/^{30}Si$ for Cu, Mo and LREE as a function of water content, whereas some decrease in the relative sensitivity factors of $^{64}Zn/^{30}Si$ and $^{208}Pb/^{30}Si$ was observed in the most hydrated glasses. We have used the observed external precision (for 37 reference samples combined) to evaluate the precision of our analyses: for hydrous glasses this corresponds to ±5–10% of the value for low H_2O concentrations (<3.87 wt%) and to ±15–20% for high H_2O concentrations samples (≥ 3.87 wt%) (electronic annex, Table EA1).

Table 1. : Major and trace element composition of two types of melt inclusions in quartz, matrix glasses and pre-eruptive and degassing rhyolitic melts

Inclusion:	**Hom2a:2a**	**Hom2a:2b**	**Hom2a:4a**	**Hom2a:4c**	**Hom2a:6b**	**Hom2a:6c**	**Hom2a:8a**	**Hom2a:10a**	**Hom2a:11c**	
Features:	**H_2O-rich**	**H_2O-poor**	**H_2O-rich**	**H_2O-poor**	**H_2O-rich**	**H_2O-rich**	**H_2O-poor**	**H_2O-poor**	**H_2O-rich**	
SiO_2 (wt%)$_{EMPA}$	73.95	77.66	75.46	77.98	74.87	75.74	78.33	77.94	75.21	
TiO_2	0.11	0.11	0.07	0.09	0.12	0.14	0.13	0.08	0.11	
Al_2O_3	11.82	13.19	11.84	13.22	11.97	11.85	13.35	13.26	12.05	
FeO[c]	0.71	0.76	0.58	0.72	0.59	0.55	0.83	0.64	0.67	
MgO	0.17	0.24	0.15	0.18	0.16	0.16	0.23	0.15	0.19	
CaO	1.02	1.21	1.02	1.22	1.11	1.08	1.24	1.11	1.03	
Na_2O	3.23	3.70	2.97	3.63	2.41	2.01	3.74	3.92	3.47	
K_2O	2.58	2.80	2.53	2.83	2.52	2.26	2.78	2.84	2.54	
Sum	93.59	99.68	94.62	99.87	93.74	93.80	100.63	99.95	95.27	
H_2O (wt%)$_{EMPA}$[a]	8.79	3.88	6.73	n.a.	n.a.	n.a.	0.88	1.24	7.11	
H_2O (wt%)$_{SIMS}$[b]	8.67	2.84	7.03	0.10	8.74	*4.29*[d]	0.10	1.06	8.31	
Zn (ppm)$_{SIMS}$	51	94	d.l.	122	51	*16*	137	101	55	
Cu	110	118	d.l.	89	100	*d.l.*	47	d.l.	d.l.	
Mo	2.0	2.0	2.0	2.1	1.8	*1.5*	2.0	2.1	1.9	

Inclusion:	**Hom2a:2a**	**Hom2a:2b**	**Hom2a:4a**	**Hom2a:4c**	**Hom2a:6b**	**Hom2a:6c**	**Hom2a:8a**	**Hom2a:10a**	**Hom2a:11c**	
Features:	**H_2O-rich**	**H_2O-poor**	**H_2O-rich**	**H_2O-poor**	**H_2O-rich**	**H_2O-rich**	**H_2O-poor**	**H_2O-poor**	**H_2O-rich**	
La	16	17	17	19	15	*11*	22	20	14	
Ce	17	18	19	22	16	*8*	26	23	14	
Pr	1.5	1.6	1.6	1.9	1.3	*0.7*	2.4	2.1	1.1	
Pb	d.l.[c]	d.l.	d.l.	16	d.l.	d.l.	14	19	d.l.	
Inclusion:	Hom2ax12a	Hom2ax13a	Hom2ax14a	Hom2b:1c	Hom2b:2d	Hom2bx1a	Rhyolitic melt[f]		Matrix glass[g]	
Features:	H_2O-poor	H_2O-poor	H_2O-poor	H_2O-rich	H_2O-rich	H_2O-poor	Pre-eruptive	Degassing	*Nn*	*Fm*
SiO_2 (wt%)$_{EMPA}$	79.54	76.73	78.65	74.94	74.61	75.29	79.7	78.1		77.20 ± 0.53
TiO_2	0.10	0.07	0.12	0.11	0.12	0.07	0.09	0.11		0.14 ± 0.08
Al_2O_3	13.31	12.65	13.16	11.68	11.91	12.64	12.0	12.7		12.66 ± 0.14
FeO[c]	0.33	0.67	0.66	0.64	0.49	0.67	0.60	0.72		1.18 ± 0.35
MgO	0.03	0.15	0.18	0.14	0.15	0.14	0.15	0.18		0.13 ± 0.05
CaO	1.17	1.09	1.15	1.13	1.05	1.11	1.03	1.13		1.22 ± 0.08
Na_2O	3.66	3.91	3.59	2.59	2.61	3.77	3.4	3.7		3.82 ± 0.19
K_2O	2.99	2.79	2.87	2.42	2.64	2.81	2.9	3.2		3.05 ± 0.08
Sum	101.13	98.06	100.37	93.67	93.56	96.50	99.9	99.9		99.41

Inclusion:	**Hom2a:2a**	**Hom2a:2b**	**Hom2a:4a**	**Hom2a:4c**	**Hom2a:6b**	**Hom2a:6c**	**Hom2a:8a**	**Hom2a:10a**	**Hom2a:11c**	
Features:	**H_2O-rich**	**H_2O-poor**	**H_2O-rich**	**H_2O-poor**	**H_2O-rich**	**H_2O-rich**	**H_2O-poor**	**H_2O-poor**	**H_2O-rich**	
H_2O (wt%)$_{EMPA}$	n.a.	n.a.	n.a.	[6.88]	[6.65]	n.a.	7.2 ± 0.9	2.0 ± 1.6		n.a.
H_2O (wt%)$_{SIMS}$	0.09	3.14	*0.07*[4]	5.11	6.15	4.34	7.3 ± 1.5	1.7 ± 1.1		1.21
Zn ppm$_{SIMS/LA-ICPMS}$[e]	94	47	*42*	44	44	30	49 ± 5	89 ± 39	n.a.	113.4 ± 20
Cu	80	31	*96*	d.l.	22	43	77 ± 48	68 ± 33	n.a.	35.6 ± 4
Mo	2.1	2.0	*1.6*	1.7	2.0	2.0	1.9 ± 0.14	2.1 ± 0.05	1.5 ± 0.3	3.1 ± 0.9
La	17	19	*12*	14	18	17	15.9 ± 1.8	18.8 ± 1.7	15 ± 0.7	12.1 ± 0.9
Ce	19	22	*9*	13	21	19	16.7 ± 3.0	21.2 ± 2.7	28 ± 1.1	30.9 ± 2.1
Pr	1.8	1.9	*0.7*	1.0	1.8	1.6	1.4 ± 0.3	1.9 ± 0.3	2.3 ± 0.12	—
Pb	14	d.l.	*d.l.*	d.l.	d.l.	d.l.	n.a.	15.7 ± 2.4	16 ± 0.6	27.6 ± 2.4
As ppm $_{LA-ICP-MS}$	n.a.	n.a.	n.a.	n.a.	n.a.	n.a.	n.a.	18.7 ± 3.5	11 ± 1.9	26.3 ± 5.1
Sb	n.a.	n.a.	n.a.	n.a.	n.a.	n.a.	n.a.	1.4 ± 0.35	1.1 ± 0.2	1.6 ± 0.5
Cd	n.a.	n.a.	n.a.	n.a.	n.a.	n.a.	n.a.	1.6 ± 1.2	0.98	2.2 ± 1.2
Au	n.a.	n.a.	n.a.	n.a.	n.a.	n.a.	n.a.	⩽*0.022*	⩽*0.022*	—

[a] H_2O (wt%)$_{EMPA}$ concentrations are determined by EMPA (Borisova et al., 2005) in H_2O-rich (H_2O ⩾ 5 wt%) and H_2O-poor (H_2O < 5 wt%) glasses of melt inclusions.
[b] H_2O (wt%)$_{SIMS}$ and trace element contents are determined by SIMS (this work); major element analyses of melt inclusions by EMPA were performed in GFZ.
[c] n.a., values are not available; d.l., values are below detection limit due to either strong drift or drop in $^{65}Cu/^{30}Si$, $^{64}Zn/^{30}Si$ signals and either strong variations in $^{208}Pb/^{30}Si$ signals upon an analysis.
[d] Low water and trace element concentrations (italized) are due to an excess of the host quartz during the SIMS analysis.
[e] Trace elements contents in inclusion glasses determined by SIMS and trace elements contents in matrix glasses determined by LA-ICP-MS.

[f] Major elements contents in pre-eruptive ($H_2O \geq 5$ wt% in inclusion glasses) and degassing ($H_2O < 5$ wt% in inclusion glasses) rhyolitic melts are after Borisova et al. (2005), average H_2O and trace element contents with standard deviations in the inclusion glasses are according to the SIMS data on Cu, Zn, Mo, Pb and LREE contents in the melt inclusions, and according to the LA-ICP-MS data on As, Sb, Cd and Au in the matrix glasses.
[g] Average major element contents in matrix glasses (22 points) with 1σ standard deviations determined by EMPA in LMTG; average trace elements contents with 1σ standard deviations determined by nanosecond (*nn*, 3 points for analysis) and femtosecond (*fm*, 6 points for analysis) LA-ICP-MS.

A quadrupole-based inductively coupled mass spectrometer (ICP-MS Elan 6000, Perkin-Elmer SCIEX), nanosecond Laser Ablation System (LSX-200, CETAC) and femtosecond Pulsar IQ Amplitude technologies were used at LMTG, Toulouse, France. The laser ablation system uses an ultraviolet Nd:YAG nanosecond laser operating at a wavelength of 266 nm in Q-switched mode (Aries et al., 2001) and the femtosecond system operates at a wavelength of 800 nm. The energy level per pulse was 6–12 mJ and the laser repetition rate was 5–10 Hz. The reference and matrix glasses were analyzed in single-point mode with a pit size diameter of 40–50 μm with the femtosecond laser and 100–140 μm with nanosecond lasers. ^{23}Na, ^{42}Ca, ^{44}Ca, ^{63}Cu, ^{65}Cu, ^{66}Zn, ^{75}As, ^{85}Rb, ^{88}Sr, ^{89}Y, ^{90}Zr, ^{93}Nb, ^{95}Mo, ^{114}Cd, ^{121}Sb, ^{133}Cs, ^{138}Ba, ^{139}La, ^{140}Ce, ^{141}Pr, ^{172}Yb, ^{181}Ta, ^{197}Au, ^{208}Pb, ^{232}Th and ^{238}U mass peaks were measured with dwell times of 10-20 ms. The acquisition time for one complete analysis was 1.5–2 min. Plasma RF power was 1200–1300 W and other operating conditions and acquisition parameters of the Perkin-Elmer Elan 6000 ICP-MS were similar to those used by Aries et al. (2001). The data obtained for all silicate glasses have been processed with the GLITTER 4.0 software package. The internal standard was ^{42}Ca because it successfully reproduces the acquired element contents in NIST 610 and 612 standards within ±10% as compared to the certified values (electronic annex, Table EA1). LA-ICP-MS determined concentrations of Zn, Mo, As, Sb, Pb, Rb, Sr, U and Ta in Macusani glass were within ±25% of the solution-mode values obtained on the bulk-rock Macusani obsidian glass. NIST 610 and 612 were used as the external standards for calibration of LA-ICP-MS analyses. Detection limits for the glass analyses were 14 ppb for Au, 0.01–0.3 ppm for Sr, Mo, Sb, REE, Y, Rb, Zr, Nb, Cs, Ba, Pb, Th, U, Ta and 0.3–5 ppm for Cu, Zn and As, Sb and Cd.

Dust-free chips of the white dacite pumice investigated by Scaillet and Evans, 1999 and Borisova et al., 2005 were cleaned in distilled water, dried and crushed to powder in an agate mortar, previously cleaned with pure quartz sand. To insure complete dissolution of zircon, a fusion—mode dissolution was chosen instead of acid dissolution. About 100 mg of pumice powder were fused together with 600 mg $LiBO_2$ as a flux. Then 100 ml of bi-distilled 10% HNO_3 were added to dissolve the fused glass. After its complete dissolution, a 10 ml aliquot of this solution was furthermore treated so that the final solution (30 ml, HNO_3 0.37 N) had a dilution factor of 1000 compared to the rock. Indium was used an internal standard. ICP-MS analyses were performed with a Perkin-Elmer Elan 6000 inductively coupled mass spectrometer equipped with a standard cross-flow nebuliser-Scott spray chamber and an automatic sampler. Between every sample the whole system was washed with a HNO_3 0.37 N solution to prevent cross-contamination and memory effects. Multi-element standard solutions were run every five samples. REE were analyzed with RSD < 5%. We used our in-house developed special procedure for oxide and hydroxide interference corrections (Aries et al., 2000) which ensures good accuracy and reproducibility as demonstrated by repeated analyses of the adapted Certified Reference Materials.

3. Results

3.1. Chemistry of the Mt. Pinatubo silicic melts

3.1.1. Chemistry of homogenized melt inclusions, matrix glasses and sulfides

Major and trace element compositions of glasses of 15 homogenized melt inclusions and groundmass are listed in Table 1. The results show excellent agreement with previous EMPA

analyses (Gerlach et al., 1996 and Borisova et al., 2005). Average SiO_2 (78.8 wt%) and Al_2O_3 (12.9 wt%) contents recalculated to the volatile-free basis in inclusion glasses (Table 1) are similar to those previously determined in melt inclusions of the same sample (79.1 wt% SiO_2 and 12.5 wt% Al_2O_3; Borisova et al., 2005). The average H_2O content (4.3 wt%) of homogenized melt inclusions determined by SIMS (Table 1) is similar to that obtained with the same technique for untreated melt inclusions (4.4 wt% H_2O; Gerlach et al., 1996). It is slightly lower than the average value found in melt inclusions previously determined with the "by-difference" technique in the same sample (5.4 wt% H_2O; Borisova et al., 2005). However, if the water contents in the H_2O-poor and H_2O-rich inclusions, as defined by Borisova et al. (2005), are averaged separately, the agreement between the SIMS and the "by-difference" data is in fact very good (for example, 1.7 vs. 2.0 and 7.3 vs. 7.2 wt%, for H_2O-poor decrepitated primary melt inclusions and H_2O-rich stable primary melt inclusions), except when the H_2O contents drops below 1 wt% (Table 1). The difference between these groups of primary inclusions is their size and the decrepitation character for the largest melt inclusions (>80 μm, Borisova et al., 2005). Major element compositions of groundmass glasses determined by EMPA in this work overlap those previously determined by Gerlach et al. (1996).

Copper and zinc concentrations are characterized by a substantial variability, both in the H_2O-rich (22–110 ppm Cu; 44–55 ppm Zn) and H_2O-poor (31–118 ppm Cu; 30–137 ppm Zn) inclusions (Table 1). Other trace elements exhibit less variable concentrations. LREE and Mo concentrations are indistinguishable in H_2O-rich (15.9 ± 1.8 ppm La; 16.7 ± 3.0 ppm Ce; 1.4 ± 0.3 ppm Pr; 1.9 ± 0.14 ppm Mo) and H_2O-poor (18.8 ± 1.7 ppm La; 21.2 ± 2.7 ppm Ce; 1.9 ± 0.3 ppm Pr; 2.1 ± 0.05 ppm Mo) inclusions within the precision of SIMS analysis. Therefore, the available data show that the trace element contents of the H_2O-rich and H_2O-poor melt inclusions overlap. Lead concentrations could be determined in the H_2O-poor inclusions only (15.7 ± 2.4 ppm Pb, Table 1). Except for volatile H_2O the decrepitation process at 13–24 MPa should not change the major and trace element contents of the primary melt inclusions (e.g., Borisova et al., 2005). Average values of matrix glass LREE, Mo and Pb concentrations by LA-ICP-MS (15 ± 0.7 ppm La; 28 ± 1.1 ppm Ce; 2.3 ± 0.12 ppm Pr; 1.5 ± 0.3 ppm Mo; 16 ± 0.6 ppm Pb) are similar to melt inclusion SIMS values (Table 1). Cu and Zn contents in the matrix glass (35.6 ± 4 ppm Cu; 113 ± 20 ppm Zn) are also similar to those of the inclusion averages (71 ± 36 ppm Cu and 73 ± 35 ppm Zn). The matrix glass analyses yield average As and Sb contents of 18.7 ± 3.5 and 1.4 ± 0.35 ppm, respectively; and one analysis of matrix glass yields 22 ± 8 ppb of Au. Based on the data on LREE, Mo and Pb we conclude that the matrix glass has trace element concentrations very close to the inclusions taken as a whole (Table 1). This indicates that syn-eruptive degassing (Borisova et al., 2005) has little influence on the trace element chemistry of the analyzed silicate glasses. Major and trace element compositions of chalcopyrite with high concentrations of Fe, Cu and Zn (30.0–30.4 at% Fe, 26–28 at% Cu and 0.67–0.76 at% Zn, respectively, Table 2) are close to those previously published by Hattori (1993).

Table 2. : Major and trace element compositions of the Mt. Pinatubo parental dacitic and the pre-eruptive rhyolitic melts and the estimated compositions of equilibrium aqueous fluids according to the available experimental partition coefficients

	Parental dacitic melt[a]	**Fluid of dacitic melt[b]**	**Pre-eruptive rhyolitic melt[c]**	**Pre-eruptive aqueous fluid[d]**	**Sulfide phases[e]**	**K_d fluid/melt[f]**
	wt%/ppm/ppb	**Calculated wt%/ppm**	**wt%/ppm/ppb**	**Calculated wt%/ppm**	**ppm**	**Experimental**
SiO_2 (wt%)	65.17	—	79.7	—	—	—
TiO_2	0.52	—	0.09	—	—	—
Al_2O_3	16.34	—	12.0	—	—	—
FeO[c]	4.16	—	0.60	—	47.26	—
MgO	2.44	*0.50*	0.15	—	—	$0.033 \times [Cl]^2$
CaO	5.22	*2.62*	1.03	—	—	$0.0804 \times [Cl]^2$
Na_2O	4.65	*5.44*	3.4	*6.37*	—	$0.468 \times [Cl]$
K_2O	1.56	—	2.9	—	—	—
H_2O (wt%)	10	—	7.3	—	—	—
Cl ppm	474 ± 33	*87672*	1033	*37935*	—	*185*
HCl (ppm)	487 ± 35	*90164*	1062	*39013*	—	—
Cl (mol/kg^{fluid})	—	*2.47*	—	*1.07*	—	—
S (ppm)	1361 ± 588	—	74	—	357,261	—
Sr (ppm)	556.7	*383*	167.6	*22*	—	$0.11 \times [Cl]^2$
Y	12.4	—	3.5	—	—	—

	Parental dacitic melt[a]	**Fluid of dacitic melt[b]**	**Pre-eruptive rhyolitic melt[c]**	**Pre-eruptive aqueous fluid[d]**	**Sulfide phases[e]**	**K_d fluid/melt[f]**
	wt%/ppm/ppb	**Calculated wt%/ppm**	**wt%/ppm/ppb**	**Calculated wt%/ppm**	**ppm**	**Experimental**
La	15.59 ± 0.37	—	15.9 ± 1.8	—	—	—
Ce	32.40 ± 1.17	—	16.7 ± 3.0	—	—	—
Pr	3.66	—	1.4 ± 0.3	—	—	—
Zn	52.9 ± 2.6	*3108*	49 ± 5	*830*	4,667	$9.4 \times [Cl]^2$
Cu	25.5 ± 13.8	*1274*	77 ± 48	*770*	264,873	$9.1 \times [Cl]$
Mo	0.908	*2*	1.9 ± 0.14	*5*	—	*2.5*
Pb	9.93 ± 1.75	*140*	15.7 ± 2.4	*44*	1,379	$2.26 \times [Cl]^2$
As	3.42 ± 0.25	—	18 ± 3.5	—	308	—
Sb (ppm)	0.33 ± 0.12	—	1.4 ± 0.35	—	—	—
Au (ppb)	6.4	*0.25*; [*38*]	22 ± 8	*0.38*; [*130*]	—	$exp\,(2.2 \times log[HCl] - 7.2)$; [*5900*]
Magmatic phases fractions (wt%)	100	—	42.8–44.7	—	0.05–2.0	—

[a] Parental dacitic melt composition is average bulk rock analyses of the Mt. Pinatubo white dacite pumice obtained in this work for Mo, Pr and Au and published data (with 1σ standard deviations) from Bernard et al., 1996, Fournelle et al., 1996, Luhr and Melson, 1996 and Pallister et al., 1996; Variable S contents in white dacite pumices are explained by secondary alteration of magmatic anhydrite (e.g., Bernard et al., 1996). Variable Cu could be due to desulfidization process; Au in ppb.

[b] Composition of aqueous fluid in equilibrium with dacitic melt is calculated according to fluid/melt partitioning of Webster (1992a) for Cl, Cl mol/kg or HCl ppm contents of the fluid and metal fluid/melt partitioning.[f]

[c] The Mt. Pinatubo pre-eruptive rhyolitic melt composition is average major and trace element composition for melt inclusions homogenized at 760 °C and 200 MPa (major elements, Cu, Zn, Pb, Mo, La, Ce and Pr, Table 1) and matrix glasses (Sr, Y, As, Sb and Au measured by LA-ICP-MS, Table 1) with standard deviations; S and Cl contents are from Borisova et al. (2005); Au in ppb; The fractions of rhyolitic glass in dacite is after Luhr and Melson, 1996 and Bernard et al., 1996.

[d] Composition of fluid in equilibrium with rhyolitic melt is determined based on fluid/melt partitioning of Webster (1992b) for Cl, [Cl] mol/kg or HCl ppm contents of the

fluid and metal fluid/melt partitioning.[f]

[e] Sulfide phase composition is chalcopyrite analyzed by EMPA in this work. The estimate of 0.05–2.0 wt% fraction of sulfides in dacite pumices is made using the data on Cu and Zn concentrations in rhyolitic melt, sulfide and the host dacite magma and the fraction of rhyolitic melt in the magma.

[f] Metal fluid/melt partitioning of Urabe (1985) for Na, Pb and Zn; Carron and LaGache (1980) for Sr; Holland (1972) for Mg and Ca; Candela and Holland (1984) for Mo and Cu based on Cu content 56 ppm of Pallister et al., 1996, Frank et al., 2002 and Hanley et al., 2005 for Au (in ppm), [Cl] (in mol/kg) and HCl (in ppm).

3.1.2. Chemistry of the bulk-rock white dacite pumices

Average major and trace element data for the bulk dacite pumices are listed in Table 2 and enrichment/depletion patterns relative to N-MORB are illustrated in Fig. 3. The new ICP-MS data for white dacite pumice yield 28.3 ppm Cu, 11.3 ppm Pb, 4.3 ppm As, 0.8 ppm Sb, 13.0 ppm La, 30.6 ppm Ce, 577.1 ppm Sr and 13.6 ppm Y. These values are in close agreement with literature data (Table 2). The Au (6.4 ppb), Mo (0.91 ppm) and Pr (3.7 ppm) concentration data are reported for the first time for the Pinatubo dacite (Table 2).

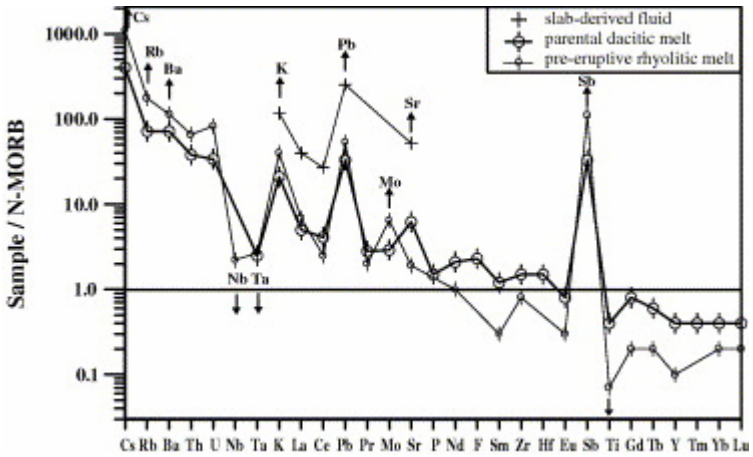

Fig. 3. N-MORB-normalized pattern of the parental dacitic melt and the pre-eruptive rhyolitic melt. Data on the composition of the dacitic melt are those of the white dacite pumices (Bernard et al., 1996, Fournelle et al., 1996, Luhr and Melson, 1996 and Pallister et al., 1996), original data for Au, Mo and Pr, (Table 2). The pre-eruptive melt composition is according to original data (Table 1 and Table 2). Enrichment in Cs, Rb, Ba, Th, U, K, Pb, Sr, Mo and Sb relative to "adjacent" REE and depletion in Ta, Nb and Ti relative to "adjacent" REE are highlighted by arrows. Normalization to N-MORB composition of Sun and McDonough (1989) is applied. ICP-MS analysis of white dacite pumice in this work yields the following trace element contents: 0.908 ppm Mo, 11.3 ppm Pb, 13 ppm La, 30.6 ppm Ce, 577 ppm Sr, and 13.6 ppm Y (and Table 2). LA-ICP-MS analysis of rhyolitic glasses of groundmass yields the following trace element contents: 98.57 ± 4.31 ppm Rb, 7.66 ± 0.4 ppm Cs, 719 ± 63 ppm Ba, 0.36 ± 0.04 ppm Ta, 5.14 ± 0.28 ppm Nb, 7.93 ± 0.35 ppm Th, 3.88 ± 0.23 ppm U, 59.17 ± 3.05 ppm Zr, 6.94 ± 0.45 ppm Nd, 0.89 ± 0.19 ppm Sm, 0.26 ± 0.05 ppm Eu, 0.75 ± 0.15 ppm Gd, 0.1 ± 0.02 ppm Tb, 0.48 ± 0.09 ppm Yb, 0.1 ± 0.02 ppm Lu (and Table 1 and Table 2).

Differences in major element contents between the bulk rock dacite and rhyolitic glasses of the matrix and inclusions are represented by Ti, Al, Fe, Mg, Ca and Na enrichment in the dacite, and Si, K enrichment in the rhyolitic glasses. In addition, Sr, Y and REE (except for La) are enriched, and Cs, Rb and Ba are depleted in the dacite relative to the inclusion and matrix glasses (Fig. 3). Au (6.4 vs. 22 ppb), Cu (28 vs. 71 ppm), Pb (10 vs. 16 ppm), Mo (0.9 vs. 2.0 ppm), As (3.4 vs. 11 ppm), and Sb (0.3 vs. 1.1 ppm) are enriched in the rhyolitic glasses relative to the bulk dacite. For Zn, the concentrations are similar.

4. Discussion

4.1. Adakite magma differentiation and metal concentration

4.1.1. Significance of the Mt. Pinatubo dacite and related rhyolitic glasses

Mt. Pinatubo is one of numerous active volcanoes in the West Central Luzon volcanic chain which are associated with eastward subduction of the Eurasian plate along the Manila trench (Fig. 1). The high Al_2O_3 (15–17 wt%), high Sr (474–608 ppm) and low Y (11–14 ppm) contents (Table 2), very low Rb/Sr (0.06–0.10) and K/Rb (264–338) ratios together with high LREE enrichment and a lack of any Eu anomaly in the Mt. Pinatubo dacites are typical features of the high-Al adakites (Drummond and Defant, 1990 and Bernard et al., 1996). Recent experimental data indicate that the most plausible mechanism for the genesis of the Mt. Pinatubo dacite magma is high-pressure fractionation of hydrous, oxidizing, primitive basalt that crystallized amphibole and garnet upon cooling (Prouteau and Scaillet, 2003). The steep negative slopes of the N-MORB-normalized patterns (Fig. 3) are consistent with the fractionation of amphibole and garnet phases. The Ta, Nb and Ti depletion in the N-MORB-normalized patterns (Fig. 3) also confirms the presence of hornblende and/or magnetite during high-pressure crystallisation.

The experimental work of Rutherford and Devine, 1996 and Scaillet and Evans, 1999 at 220 MPa (which is in the range of 190 ± 50 MPa, the total pressure of dacite magma crystallization just prior to eruption, Borisova et al., 2005) has essentially reproduced both the phase assemblage and composition of the Mt. Pinatubo dacites, with the exception of the rare high-Al hornblende cores and calcic plagioclase which together represent <1% of the phenocryst volume (Prouteau and Scaillet, 2003). These data imply that the dacite magma arrived in a nearly molten state in the pre-eruptive reservoir where major crystallization occurred (e.g., Prouteau et al., 1999 and Prouteau and Scaillet, 2003). We suggest, therefore, that the bulk composition of the dacite pumice closely reflects the chemistry of the parental dacitic melt. In the same way, the composition of rhyolitic melt inclusions and matrix glass reflects the chemistry of the residual melt which results from crystallization of the dacite at its pre-eruptive storage level. These parental–residual relationships offer the opportunity to discuss the behaviour of metals during differentiation of adakitic magma.

4.1.2. Metal concentrations

The concentrations of ore metals in the residual rhyolitic melt (Au = 22 ± 8 ppb, and average Cu = 71 ± 36 ppm, Pb = 16 ± 2 ppm, Mo = 2.0 ± 0.1 ppm, As = 11 ± 1.9 ppm, Sb = 1.1 ± 0.2 ppm) are by a factor of 2–3 higher than those in the parental dacitic melt (Au ~ 6.4 ppb, Cu ~ 28 ppm, Pb = 10 ± 1.8 ppm, Mo ~ 0.9 ppm, As ~ 3.4 ppm and Sb ~ 0.33 ppm). Note however that the Zn concentration in the pre-eruptive rhyolitic melt (73 ± 35 ppm) is not distinguishable within error from that of the parental dacitic melt (53 ± 3 ppm). Overall, these data reflect the incompatible behaviour of ore metals during dacite magma crystallization and differentiation (Fig. 4). The increase in Au, Cu, Pb, Mo, As and Sb in silicic melts is accompanied by an increase in chlorine content (474–1033 ppm) and a dramatic decrease in sulphur contents (1361–74 ppm) during crystallization of the dacite magma (Fig. 4).

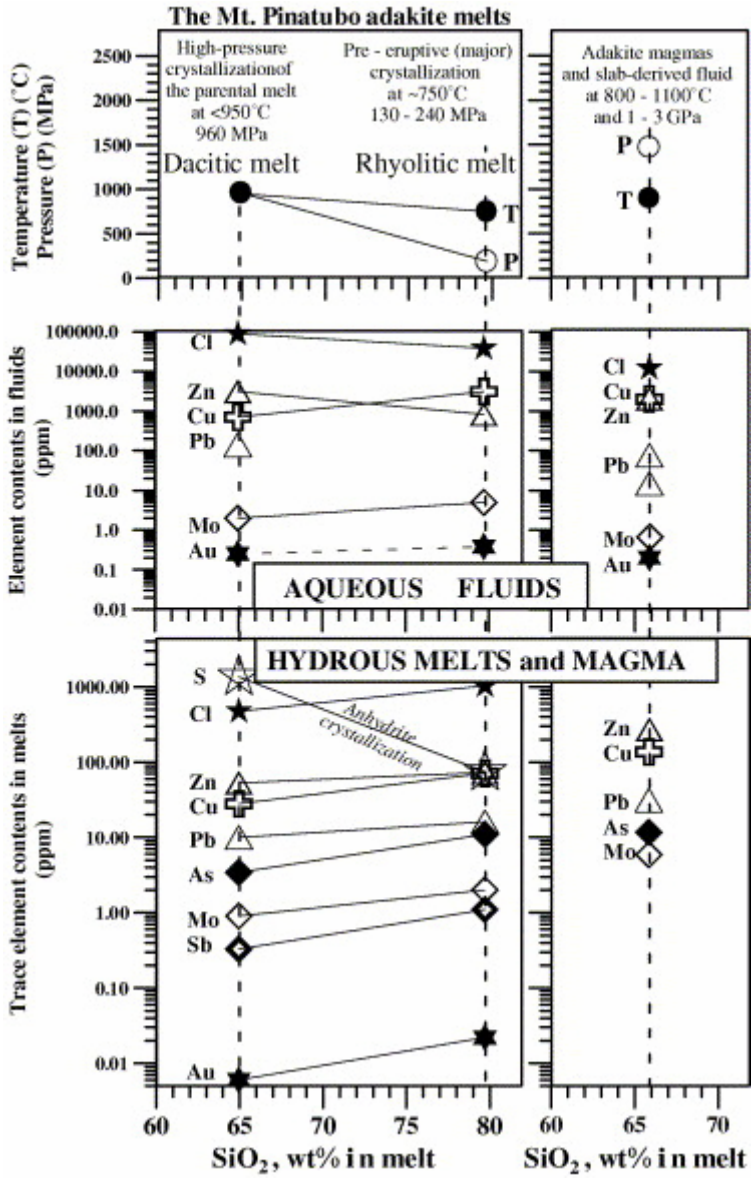

Fig. 4. Chemistry of hydrous melts and equilibrium aqueous fluids. Temperature (°C)–pressure (MPa) conditions of the Mount Pinatubo magma crystallization, together with trace element compositions in co-existing melts and fluids versus SiO_2 contents in melts. The high-pressure crystallization stage of the parental dacitic melt at 950 °C, 960 MPa and the pre-eruptive crystallization of the rhyolitic melt at 750 °C and total pressure of 190 ± 50 MPa are shown. Adakite magma and slab-derived fluid at 800–1100 °C and 1–3 GPa are illustrated. Trace element data of the melts and fluids are from Table 2 and Table 3.

Highly oxidizing conditions during magma differentiation are favorable for concentrating ore metals in the residual melt, because high oxygen fugacity eliminate the early segregation of sulfides (e.g., pyrrhotite) which may act as a sink for Cu, Zn and Au (e.g., Candela, 1989). At least two phases controlled the ore metals chemistry of the dacite magma at the pre-eruptive conditions, chalcopyrite ($\leq$2 wt%) with high concentrations of Cu, Zn and rhyolitic melt (43–45 wt%) which forms the groundmass (Table 2). Chalcopyrite globules occur as multiphase inclusions in dacite phenocrysts (Fig. 2) and resorbed chalcopyrite segregations are found in the rhyolitic glass matrix (Table 2). The magma differentiation occurred at oxidizing conditions, above NNO + 1, at conditions where sulfate species [SO_4] dominate over sulfide complexes $[S]^{2-}$ in the hydrous melts (Fig. 5). This significantly reduces sulfide phase

formation and fractionation. A limited amount of titanomagnetite (<4 wt%), crystallized under the Mt. Pinatubo high-pressure conditions (Prouteau and Scaillet, 2003), which may explain why the dacite magma was finally enriched in Zn and Mo (Fig. 3).

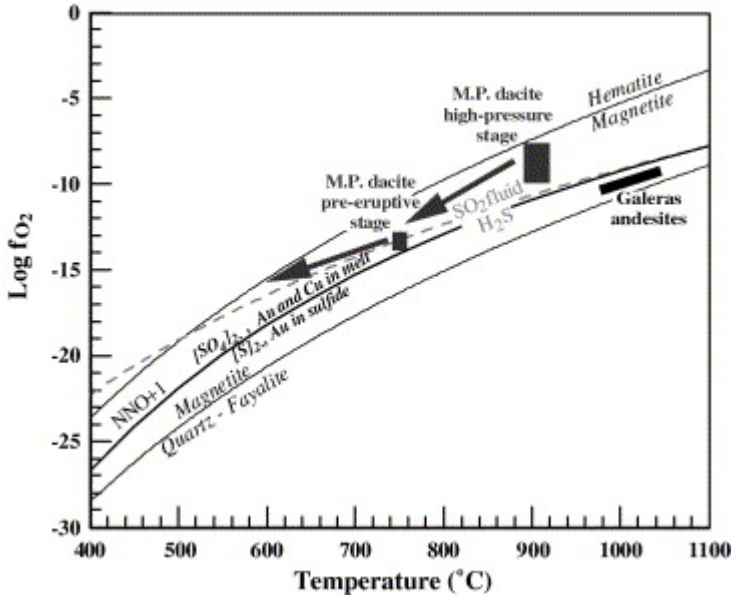

Fig. 5. Log f_{O2} versus temperature (°C) showing redox conditions for the Mt. Pinatubo crystallization stages. The high-pressure redox conditions are according to Prouteau and Scaillet (2003) and the pre-eruptive redox conditions are from Borisova et al., 2005 and Scaillet and Evans, 1999. T–f_{O2} conditions for the Galeras andesites related to Au/Cu deposits are from Goff et al. (1994). Thin solid curves, hematite–magnetite and magnetite–quartz–fayalite equilibria; thick solid curve, f_{O2} corresponding to NNO + 1. This curve also delimits the predominance of sulfate $[SO_4]^{2-}$ versus sulfide $[S]^{2-}$ in the hydrous silicic melts (Carroll and Rutherford, 1987, Andersen and Lindsley, 1988 and Clemente et al., 2004). Au, Cu in melt versus Au in sulfide boundary are according to Mungall (2002) and corresponding to NNO + 1. Dashed curve corresponds to a 1:1 SO_2 and H_2S ratio in the fluid, according to the reaction $H_2S + 1.5O_2 = SO_2 + H_2O$ (Carroll and Rutherford, 1987).

4.1.3. Constraints on the chemistry of aqueous fluids

Although an aqueous fluid phase was trapped in rare inclusions in quartz (Pasteris et al., 1996), most fluid inclusions were decrepitated and the fluid was not retained (Fig. 2). The chemistry of the primary fluid (e.g., SO_2, H_2S, HCl, trace element contents) should depend on the chemistry of the associated hydrous melts and pressure-temperature and redox conditions (P–T–f_{O2}). The high Cl concentrations, above 500–1000 ppm, in the silicic melts imply these melts were close to saturation with chlorine (Metrich and Rutherford, 1992). The experimentally established empirical correlations between Cl mol% or HCl wt% contents and trace element concentrations in magmatic fluids (e.g., Candela and Holland, 1984, Urabe, 1985 and Frank et al., 2002) put reliable constraints on Cl content in the fluid. We used data on Cl contents in melts (Table 2) and available experimental data on Cl partitioning at 800–1000 °C and 200–800 MPa for silicic melts (Table 2; Metrich and Rutherford, 1992, Webster, 1992a and Webster, 1992b). The parental dacitic melt and the pre-eruptive rhyolitic melt are highly peraluminous with A/NK = Al/(Na + K) of 1.5–1.8 and N/NK = Na/(Na + K) of 0.6–0.7 mol%. Unfortunately, no experimental data exist on the Cl partitioning for such melts. We assume Cl partitioning for the parental dacitic melt to be similar to that of subaluminous melts with lower A/NK (1.02–1.04) and similar N/NK (0.67–0.68) at 800 °C/800 MPa and Cl_{melt} contents of 300–700 ppm (Webster, 1992a) and D_{Cl} (D_{Cl} = concentration of Cl in

fluid/concentration of Cl in melt) to be equal to 185 (Table 2). These data yield 2.5 mol/kg of chloride in the fluid in equilibrium with the parental dacitic melt at 800 °C and 800 MPa. Similarly, we expect Cl concentrations in the pre-eruptive fluid in equilibrium with the residual rhyolite melt to be similar to those of peraluminous melts with lower A/NK (1.2) and similar N/NK (0.7) (at 800 °C/210 MPa and Cl_{melt} contents 1180 ppm; Webster, 1992b) and to be equal to ~1.1 mol/kg. Thermodynamic calculations indicate that $SO_2/H_2S/HCl$ species existed in comparable amounts in the Mt. Pinatubo pre-eruptive fluid (e.g., Gerlach et al., 1996 and Scaillet et al., 1998). The soft chalcophile metals (Au, Cu) form much more stable complexes with soft ligands like HS^- than with moderately hard Cl^- and OH^-/H_2O in aqueous fluids (e.g., Pokrovski et al., 2005). However, the abundant anhydrite crystallization in melt and fluid (e.g., Pasteris et al., 1996) should result in a decrease of the fluid-phase sulfur contents, causing Cu, Au, Pb and Zn complexation with the far more abundant Cl^- in the pre-eruptive fluid, whereas As, Sb and Mo are expected to form soluble hydroxide complexes (e.g., Wood and Samson, 1998, Pokrovski et al., 2005 and Pokrovski et al., 2002).

High-Al adakitic magmas related to Au/Cu and Cu/Mo mineralization are peraluminous (González-Partida et al., 2003, Reich et al., 2003, Qu et al., 2004 and Whalen et al., 2004). Most of these magmas contain early phenocrysts of hydrous minerals such as hornblende and biotite, implying early magma saturation with an aqueous fluid (Sajona and Maury, 1998). The peraluminous compositions of the hydrous dacitic and rhyolitic melts saturated with an aqueous fluid suggest partitioning for Au, Cu, Zn, Pb and Mo in favor of the fluid phase (Candela and Holland, 1984, Urabe, 1985, Hoosain and Baker, 1996 and Hanley et al., 2005). To estimate Au, Cu, Zn, Pb, Mo and Na contents in aqueous fluids in equilibrium with the Mt. Pinatubo pre-eruptive rhyolitic and the parental dacitic melts, we used the available experimental partitioning coefficients for synthetic melts at 750–800 °C/140–200 MPa for the pre-eruptive rhyolitic melt, and at 800–1250 °C/350–900 MPa for high-pressure dacitic melt (Fig. 4, Table 2). Our estimations show that the Mt. Pinatubo aqueous fluids could contain 0.3–0.4 ppm of Au, 770–1300 ppm of Cu, 830–3100 ppm of Zn and 44–140 ppm of Pb, 2–5 ppm of Mo, and 6–11 wt% of NaCl (Table 2). Higher Au fluid contents (37–130 ppm) could be obtained using partitioning coefficients of Hanley et al. (2005) for a peraluminous system. Because at least 100–500 Mt of H_2O was liberated from the pre-eruptive magma as aqueous fluid (Gerlach et al., 1996), the calculated fluid composition suggests that the pre-eruptive fluid might have extracted a minimum of 15×10^5 t of Cu and 100 t of Au from the differentiated dacite magma. Provided that metal transport and precipitation mechanisms are efficient, the estimated Au and Cu amounts are sufficient to form a typical porphyry-type deposit and thus demonstrate that the degassing adakitic magma is likely to be the primary source for ore metals in porphyry–epithermal environments of subduction zones.

4.2. Role of slab-derived fluid in defining the geochemistry of the Mt. Pinatubo adakite melts

The very high sulfur content of the Mt. Pinatubo dacite pumices (reaching up to 2200 ppm, Bernard et al., 1991), high Se and Se/S ratio in primary sulfides of the dacites (Hattori, 1993 and Hattori, 1996) indicate that a component enriched in S and Se was involved in the genesis of the dacite. High Se/S ratios are observed in marine sediments (Goldschmidt, 1954) and the involvement of subducted sediments in the genesis of the Mt. Pinatubo dacite is also confirmed by Be isotope signatures (Bernard et al., 1996). Moreover, high Cl contents in the bulk dacitic and rhyolitic melts (Table 2), and in apatite inclusions (Borisova et al., 2005) strongly support an involvement of subducted components (sediments or metabasalts altered with seawater, Ito et al., 1983) in the genesis of the Mt. Pinatubo dacitic magma. Water

contents of the Mt. Pinatubo primary melts could be as high as 10–15 wt%, provided the melt saturation with an aqueous fluid occurs at high-pressure conditions (Fig. 4); such high H_2O contents imply water derivation from the dehydrated oceanic slab.

The high Au contents (6.4 ppb) of the Mt. Pinatubo dacitic pumices relative to regular calc-alkaline magmas (maximum of 2–3 ppb Au; Connors et al., 1993 and Polvé et al., 2004), along with the existence of strong positive anomalies of Sb, Pb and Mo relative to "adjacent" REE in the N-MORB-normalized patterns of the bulk dacite pumices and rhyolitic melt (Fig. 3), clearly demonstrate an enrichment of the Mt. Pinatubo adakitic magma in these ore metals. Sulfide melt or mineral phases are the main sink for trace chalcophile metals like Au, Cu, Zn and Pb. However, high Au and associated metals contents in dacite pumices and rhyolitic melts (Table 2) suggest that sulfide phases must be absent from their sources, and possible interactions with the overlying mantle wedge should be limited (e.g., Mungall, 2002). The high Pb/Ce, Mo/Ce, As/Ce and Sb/Ce ratios in the pre-eruptive rhyolitic and the parental dacitic melts (Table 2) are close to those of subduction zone magmas near the volcanic front (Noll et al., 1996) where the possible interaction with the mantle wedge is expected to be minimal (McCulloch and Gamble, 1991).

The calculated Pb/Ce and As/Ce ratios in the oceanic slab and adakitic magmas (Table 3) suggest that, in addition to the slab, a fluid phase is likely to be responsible for the observed ore metal enrichment in the adakitic magmas. Indeed, the enrichment in Pb, Mo, As and Sb relative to Ce in the melts is likely to be a result of fluid-melt fractionation rather than crystal-melt fractionation (Noll et al., 1996). Pb and Cu enrichment relative to REE and Y is documented in slab-derived fluid during dehydration of subducting oceanic crust (e.g., Kogiso et al., 1997). Such a fluid derived from the dehydrated oceanic slab is likely to be important in the ore metal enrichment of the adakitic magmas. Because of the highly oxidizing conditions during adakite magma differentiation which destabilize sulfide phases, these metals are easily mobilized likely in the form of chloride complexes by Cl-bearing aqueous fluids (Keppler and Wyllie, 1991, Stolper and Newman, 1994, Keppler, 1996, Frank et al., 2002 and Pokrovski et al., 2005) derived from descending, dehydrated oceanic crust. Moreover, the SO_2 ligand which becomes the dominant sulfur species at the expense of H_2S in the oxidized fluid might also form soluble complexes with chalcophile metals and, thus, further facilitate their mobility.

To estimate major and trace element compositions of the slab-derived fluid, we used the available data on trace element partitioning between slab and fluid, and eclogite mineral and fluid (Table 3). The estimated composition of the slab-derived fluid is enriched in Pb and alkaline earth elements relative to REE (Fig. 3). The calculated contents of Sr, Au, Cu, Zn, Pb and Mo in the slab-derived fluid overlap those of the aqueous fluid in equilibrium with the Mt. Pinatubo dacitic magma at high-pressure conditions (Fig. 4, Table 2 and Table 3). These findings support the idea that the saturation of the Mt. Pinatubo adakitic melt with metal-bearing fluid promoted the enrichment of the adakitic magmas in gold and associated metals and H_2O (Table 2). $^{87}Sr/^{87}Sr$ ratios approaching 0.704 in the Mt. Pinatubo adakitic magmas (e.g., Bernard et al., 1996) are typical of the oceanic slab (McCulloch and Gamble, 1991), and their high Sr/Y ratio (between 45 and 48) could indicate that the chemistry of these magmas was controlled by supercritical fluids rich in Sr and derived directly from the dehydrated oceanic slab.

Table 3. : Major and trace element compositions of subducting oceanic slab (MORB and sediments), slab-derived fluid, and adakite magma

	MORB		**GLOSS**[c]	**Slab**[d]	**Enrichment factor (relative to MORB)**	**Model slab-derived fluid**[e]	**Enrichment factor (relative to MORB)**	**Adakite magma**[f]
	Unaltered[a]	**Altered**[b]						
	Wt%/ppm/ppb		**Wt%/ppm/ppb**	**Wt%/ppm/ppb**		**Wt%/ppm**		**Wt%/ppm**
SiO_2 (wt%)	50.45	52.30	58.57	50.95	*1.00*	—	—	65.88
TiO_2	1.62	2.25	0.62	1.60	*0.99*	—	—	0.30
Al_2O_3	15.26	17.95	11.91	15.23	*1.00*	—	—	17.49
FeO[c]	10.43	—	5.21	—	—	—	—	2.88
MgO	7.58	13.23	2.48	8.08	*1.07*	—	—	1.26
CaO	11.30	13.30	5.95	11.13	*0.98*	—	—	4.79
Na_2O	2.68	4.48	2.43	2.76	*1.03*	—	—	4.25
K_2O	0.11	8.16	2.04	0.61	*5.55*	5.0	*45*	1.44
H_2O (wt%)	0.01	5.8	7.29	0.66	*66*	95	*9500*	~15
Cl (ppm)	—	—	—	—	—	11,900	—	—
Sr (ppm)	120	350	327	142	*1.2*	223–2933	*24*	760
Y	30	59	29.8	31	*1.0*	0.03–33	*1.1*	3
La	2.8–3.9	11	28.8	6	*2.0*	2.7–99	*35*	9.3
Ce	8.3–12	28	57.3	14	*1.7*	6.3–200	*24*	17.1
Zn	72–95	135	86.4	76–97	*1.3*	2070	*29*	104

	MORB		GLOSS[c]	Slab[d]	Enrichment factor (relative to MORB)	Model slab-derived fluid[e]	Enrichment factor (relative to MORB)	Adakite magma[f]
	Unaltered[a]	Altered[b]						
	Wt%/ppm/ppb		Wt%/ppm/ppb	Wt%/ppm/ppb		Wt%/ppm		Wt%/ppm
Cu	75	295	75.0	86	*1.2*	1996	*27*	171
Mo	2.1	12	0.6	3	*1.4*	0.44	*0.2*	7
Pb	0.4–0.7	55	19.9	4	*10*	16–400	*1000*	33
As	2	5	10.3	2.6	*1.3*	7.3	*3.7*	11
Sb (ppb)	17–74	7259	400	600	*35*	450	*26*	1800
Au (ppb)	3.2–8.7	0.2–0.7	1.1–3.1	1.1–4.1	*1.3*	~200	*62*	—
Sr/Y	4	6	11	5	—	97,766	—	253
Pb/Ce	0.03–0.06	2	0.3	0.3	—	63	—	1.9
Mo/Ce	0.18–0.25	0.4	0.01	0.18	—	0.21	—	0.4
As/Ce	0.17–0.24	0.18	0.07	0.16	—	3.5	—	0.6

[a] Average unaltered MORB data are from: Sun et al. (2004) for Au; Hertogen et al. (1980) for Zn, Sb and Au; Doe (1994) for Cu, Pb; Jochum and Verma (1996) for Sb, Pb, Sr, Y and LREE; Hofmann (1988) for major elements, La, Ce; Onishi and Sandell (1955) for As; Au and Sb are in ppb.
[b] Maximal contents of major and trace elements in altered MORB and MORB glasses are after Alt and Emmermann, 1983, Frey et al., 1974, Humphris and Thompson, 1978a, Humphris and Thompson, 1978b and Staudigel et al., 1981 for major elements, Cu, Sr, Y, LREE and Pb; Jochum and Verma (1996) for La, Ce, Pr, Pb and Sb; Pichler et al. (1991) for Mo, Sr; Böhlke et al. (1981) for H_2O, Cu and Zn; Onishi and Sandell (1955) for As; Nesbitt et al. (1987) for Au; Au and Sb in ppb.
[c] The global subducting sediment composition (GLOSS) is after Plank and Langmuir (1998); model sediment data for As, Sb and Mo (in ppm) are from Noll et al., 1996 and Onishi and Sandell, 1955; Au (in ppb) is after Crocket et al. (1973).
[d] The slab composition is estimated as 5 wt% sediment (GLOSS), 5 wt% altered MORB and 90 wt% unaltered MORB; enrichment factors is maximal ratios of slab concentrations to those of fresh MORB.
[e] Composition of slab-derived fluid (or supercritical fluid) is after Tatsumi and Kogiso (1997) for Cl, H_2O, Na_2O, K_2O, Sr, Y and Pb; the fluid composition is calculated after slab composition and slab/fluid partitioning for Pb, Sr, Y, La and Ce of Ayers (1998) and eclogite/fluid partitioning of Brenan et al. (1995) for Pb and Sr; H_2O-rich component

of Stolper and Newman (1994) for Cl, Cu, Zn and Pb is also used; Au (ppb) contents in amphibolite-derived fluid are after Loucks and Mavrogenes (1999); As, Sb, Mo, Mo/Ce, As/Ce and Sb/Ce are after Noll et al. (1996); enrichment factors is maximal ratios of slab-derived fluid concentrations to those of fresh MORB. [f] Adakite magma composition is major and trace element (La, Ce, Sr and Y) composition of Cenozoic adakites after Drummond and Defant (1990) and H_2O content is after Prouteau et al. (1999); Chalcophile element contens are average of those of young adakite-like magmas related to ore deposits (González-Partida et al., 2003 and Qu et al., 2004).

4.3. Concluding remarks: Ore-forming potential of adakite magmatism

Oxidizing conditions above NNO + 1 during the high-pressure and pre-eruptive crystallization stages of the Mt. Pinatubo magma caused the predominance of sulfate over sulfide in the hydrous magmas. In turn, this limited the segregation of chalcopyrite and promoted Au- and associated Cu, Zn, Pb, As and Sb-enrichment in the residual adakite melts. A limited amount of titanomagnetite crystallized under the Mt. Pinatubo high-pressure conditions (Prouteau and Scaillet, 2003), explaining why the adakite magma was finally enriched in Zn and Mo (e.g., Hedenquist and Lowenstern, 1994).

The Mt. Pinatubo hydrous adakite melts were fluid-saturated and had peraluminous compositions with A/NK > 1.0. Other high-Al adakitic magmas related to Au/Cu and Cu/Mo mineralization are peraluminous as well. Most of these magmas contain early phenocrysts of hydrous minerals such as hornblende and biotite, implying early magma saturation with an aqueous fluid (Sajona and Maury, 1998). The peraluminous composition of the adakitic magmas favors the concentration of metal into an aqueous fluid phase. Although the soft chalcophile metals (Au, Cu) are known to form very stable complexes with reduced sulfur ligands (SO_2, H_2S), the effective scavenging of sulfur from melt and fluid due to abundant anhydrite crystallization rendered sulfide complexes less abundant than those with chloride which was present at much higher concentrations. Thus, the aqueous chloride-rich fluids liberated upon magma differentiation could have efficiently extracted hundreds of tones of metals with the potential to create a hydrothermal ore deposit (auriferous porphyry copper deposit or epithermal gold veins), provided that the residual magma was not erupted and that the necessary conditions for subsequent ore deposition prevailed (e.g., Loucks and Mavrogenes, 1999).

In the Philippines adakitic magmas related to Au/Cu deposits are located in the volcanic fronts of the subducting zones. The petrogenesis of the adakitic magmas was largely controlled by fluid-present melting of the subducting slab; and their location in the volcanic front is likely due to liberation of slab-derived aqueous fluids. Thus, the Mt. Pinatubo adakitic magmas are enriched in H_2O, Au, Cu, Zn, Pb, Mo, As, Sb, Sr, LREE and Cl due to an important contribution of deep slab-derived fluids.

Acknowledgments

G.S. Pokrovski is thanked for assistance and discussions. We thank M. Cathelineau, C. Marignac, E.H. Oelkers, G. Prouteau, F. Poitrasson, S. Salvi for discussions and insightful suggestions which significantly improved the manuscript. We thank M.R. Frank, J. Hanley and R.J. Goldfarb for constructive reviews and very helpful comments. The careful editorial handling of Edward M. Ripley helped clarify the manuscript. We thank Fabienne de Parseval for sample preparation for EMPA, SIMS and LA-ICP-MS. Ph. de Parseval, Th. Aigouy, O. Appelt and I. Schäpan are thanked for assistance during EMPA and SIMS analyses at LMTG and GFZ. We thank J. Koepke of the University of Hannover for preparing the hydrated glass samples used for our SIMS calibrations. This work has been supported by a post-doctoral fellowship from the French Ministry of Scientific Researches (A.B., 2005) and by CNRS grant through the GDR "Transmet" (A.B. and M.P. 2002–2005).

References

Alt and Emmermann, 1983 Alt J.C., Emmermann R., 1983, *Geochemistry of Hydrothermally Altered Basalts: Deep Sea Drilling Project Hole 504B*, Leg 83, Init. Rep. DSDP, Washington, DC, pp. 249–262.

Andersen and Lindsley, 1988 D.J. Andersen and D.H. Lindsley, Internally consistent solution model for Fe–Mg–Mn–Ti oxides, *Am. Mineral.* **73** (1988), pp. 714–726.

Aries et al., 2000 S. Aries, M. Valladon, M.B. Polvé and B. Dupré, A routine method for oxide and hydroxide interference corrections in ICP-MS chemical analysis of environmental and geological samples, *Geostand. Newslett.* **24** (2000), pp. 19–31.

Aries et al., 2001 S. Aries, M. Motelica-Heino, R. Freydier, Th. Grezes and M. Polvé, Direct determination of lead isotope ratios by laser ablation-inductively coupled plasma-quadrupole mass spectrometry in lake sediment samples, *Geostand. Newslett.* **25** (2001), pp. 387–398.

Ayers, 1998 J.C. Ayers, Trace element modelling of aqueous fluid—peridotite interaction in the mantle wedge of subduction zones, *Contrib. Mineral. Petrol.* **132** (1998), pp. 390–404.

Bernard et al., 1991 A. Bernard, D. Demaiffe, N. Mattielli and R.S. Punongbayan, Anhydrite-bearing pumices from mount pinatubo: further evidence for the existence of sulphur-rich silicic magmas, *Nature* **354** (1991), pp. 139–140.

Bernard et al., 1996 A. Bernard, U. Knittel, B. Weber, D. Weis, A. Albrecht, K. Hattori, J. Klein and D. Oles, Petrology and geochemistry of the 1991 eruption products of Mount Pinatubo. In: Ch.G. Newhall and R.S. Punongbayan, Editors, *Fire and Mud. Eruptions and Lahars of Mount Pinatubo, Philippines*, University of Washington Press, Seattle (1996), pp. 767–798.

Böhlke et al., 1981 J.K. Böhlke, J. Honnorez, B.-M. Honnorez-Guerstein, K. Muehlenbachs and N. Petersen, Heterogeneous alteration of the upper oceanic crust: correlation of rock

chemistry, magnetic properties, and O isotope ratios with alteration patterns in basalts from site 396B, DSDP, *J. Geophys. Res.* **86** (1981) (B9), pp. 7935–7950.

Borisova et al., 2005 A.Yu. Borisova, M. Pichavant, J.-M. Beny, O. Rouer and J. Pronost, Constraints on dacite magma degassing and regime of the June 15, 1991, climactic eruption of Mount Pinatubo (Philippines): new data on melt and crystal inclusions in quartz, *J. Volcanol. Geotherm. Res.* **145** (2005), pp. 35–67.

Brenan et al., 1995 J.M. Brenan, H.F. Shaw, F.J. Ryerson and D.L. Phinney, Mineral–aqueous fluid partitioning of trace elements at 900 °C and 2.0 GPa: constraints on the trace element chemistry of mantle and deep crustal fluids, *Geochim. Cosmochim. Acta* **59** (1995), pp. 3331–3350.

Candela, 1989 P.A. Candela, Ore deposits associated with magmas. In: J.A. Whitney and A.J. Naldrett, Editors, *Rev. Econ. Geol.* **vol. 4**, Soc. Econ. Geol., Littleton, Colorado (1989), pp. 202–232.

Candela and Holland, 1984 P.A. Candela and H.D. Holland, The partitioning of copper and molybdenum between silicate melts and aqueous fluids, *Geochim. Cosmochim. Acta* **48** (1984), pp. 373–380. Abstract

Carroll and Rutherford, 1987 M.R. Carroll and M.J. Rutherford, The stability of igneous anhydrite: experimental results and implications for sulfur behaviour in the 1982 El Chichon trachyandesite and other evolved magmas, *J. Petrol.* **28** (1987), pp. 781–801.

Carron and LaGache, 1980 J.P. Carron and M. LaGache, Etude expérimentale du fractionnement des éléments Rb, Cs, Sr et Ba entre feldspaths alcalins, solutions hydrothermales et liquides silicates dans le système Q.Ab.Or.H_2O à 2 kbar entre 700 et 800 °C, *Bull. Miner.* **703** (1980), pp. 571–578.

Clemente et al., 2004 B. Clemente, B. Scaillet and M. Pichavant, The solubility of sulphur in hydrous rhyolitic melts, *J. Petrol.* **45** (2004), pp. 2171–2196.

Connors et al., 1993 K.A. Connors, D.C. Noble, S.D. Bussey and S.I. Weiss, Initial gold contents of silicic volcanic rocks: bearing on the behavior of gold in magmatic system, *Geology* **21** (1993), pp. 937–940.

Crocket et al., 1973 J.H. Crocket, J.D. Macdougall and R.C. Harriss, Gold, palladium and iridium in marine sediments, *Geochim. Cosmochim. Acta* **37** (1973), pp. 2547–2556.

Defant and Drummond, 1990 M.J. Defant and M.S. Drummond, Derivation of some modern arc magmas by melting of young subducted lithosphere, *Nature* **347** (1990), pp. 662–665.

Drummond and Defant, 1990 M.S. Drummond and M.J. Defant, A model for trondhjemite–tonalite–dacite genesis and crustal growth via slab melting: Archean to modern comparisons, *J. Geophys. Res.* **95** (1990) (B13), pp. 21503–21521.

Doe, 1994 B.R. Doe, Zinc, copper, and lead in mid-ocean ridge basalts and the source rock control on Zn/Pb in ocean-ridge hydrothermal deposits, *Geochim. Cosmochim. Acta* **58** (1994), pp. 2215–2223.

Fournelle et al., 1996 J. Fournelle, R. Carmody and A.S. Daag, Anhydrite-bearing pumices from the June 15, 1991, eruption of Mt. Pinatubo: geochemistry, mineralogy, and petrology. In: Ch.G. Newhall and R.S. Punongbayan, Editors, *Fire and Mud. Eruptions and Lahars of Mt. Pinatubo, Philippines*, University of Washington Press, Seattle (1996), pp. 845–863.

Frank et al., 2002 M.R. Frank, P.A. Candela, P.M. Piccoli and M.D. Glascock, Gold solubility, speciation, and partitioning as a function of HCl in the brine-silicate melt-metallic gold system at 800 °C and 100 MPa, *Geochim. Cosmochim. Acta* **66** (2002), pp. 3719–3732.

Frey et al., 1974 F.A. Frey, W.B. Bryan and G. Thompson, Atlantic Ocean floor: geochemistry and petrology of basalts from legs 2 and 3 of the Deep-Sea Drilling Project, J, *Geophys. Res.* **79** (1974), pp. 5507–5527.

Gerlach et al., 1996 T.M. Gerlach, H.R. Westrich and R.B. Symonds, Pre-eruption vapor in magma of the climactic Mount Pinatubo eruption: Source of the giant stratospheric sulfur dioxide cloud. In: Ch.G. Newhall and R.S. Punongbayan, Editors, *Fire and Mud. Eruptions and Lahars of Mount Pinatubo, Philippines*, University of Washington Press, Seattle (1996), pp. 415–434.

Goff et al., 1994 F. Goff, J.A. Stimac, A.C.L. Larocque, J.B. Hulen, G.M. McMurtry, A.I. Adams, M.A. Roldán, P.E. Trujillo, D. Counce Jr., S.J. Chipera and D. Mann, Gold degassing and deposition at Galeras Volcano, Colombia, *GSA Today* **4** (1994), pp. 243–247.

Goldschmidt, 1954 V.M. Goldschmidt, Geochemistry. In: A. Muir, Editor, Clarendon Press, Oxford (1954), p. 730.

González-Partida et al., 2003 E. González-Partida, G. Levresse, A. Carrillo-Chávez, A. Cheilletz, D. Gasquet and D. Jones, Paleocene adakite Au–Fe bearing rocks, Mezcala, Mexico: evidence from geochemical characteristics, *J. Geochem. Explor.* **80** (2003), pp. 25–40.

Hanley et al., 2005 J.J. Hanley, T. Pettke, J.E. Mungall and E.T.C. Spooner, The solubility of platinum and gold in NaCl brines at 1.5 kbar, 600 to 800 °C: a laser ablation ICP-MS pilot study of synthetic fluid inclusions, *Geochim. Cosmochim. Acta* **69** (2005), pp. 2593–2611.

Hattori, 1993 K. Hattori, High-sulfur magma, a product of fluid discharge from underlying mafic magma: evidence from Mount Pinatubo, Philippines, *Geology* **21** (1993), pp. 1083–1086.

Hattori, 1996 K. Hattori, Occurrence and origin of sulfide and sulfate in the 1991 Mt. Pinatubo Eruption Products. In: Ch.G. Newhall and R.S. Punongbayan, Editors, *Fire and Mud. Eruptions and Lahars of Mt. Pinatubo, Philippines*, University of Washington Press, Seattle (1996), pp. 807–824.

Hedenquist and Lowenstern, 1994 J.W. Hedenquist and J.B. Lowenstern, The role of magmas in the formation of hydrothermal ore deposits, *Nature* **370** (1994), pp. 519–527.

Hertogen et al., 1980 J. Hertogen, M.-J. Janssen and H. Palme, Trace elements in ocean ridge basalt glasses: Implications for fractionations during mantle evolution and petrogenesis, *Geochim. Cosmochim. Acta* **44** (1980), pp. 2125–2143.

Hervig, 1996 R.L. Hervig, Analyses of geological materials for boron by secondary ion mass spectrometry. In: E.S. Grew and L.M. Anovitz, Editors, *Reviews in Mineralogy* **33**, Mineral Soc. Am., Washington, DC (1996), pp. 789–803.

Hofmann, 1988 A.W. Hofmann, Chemical differentiation of the Earth: the relationship between mantle, continental crust, and oceanic crust, *Earth Planet. Sci. Lett.* **90** (1988), pp. 297–314.

Holland, 1972 H.D. Holland, Granites, solutions, and base metal deposits, *Econom. Geol.* **67** (1972), pp. 281–301.

Hoosain and Baker, 1996 L. Hoosain and D.R. Baker, Solubility of gold in two granitic melts and its partitioning between sulfides and melt, *GAC-MAC Program Abstr.* **21** (1996), pp. A–45.

Humphris and Thompson, 1978a S.E. Humphris and G. Thompson, Hydrothermal alteration of oceanic basalts by seawater, *Geochim. Cosmochim. Acta* **42** (1978), pp. 107–125.

Humphris and Thompson, 1978b S.E. Humphris and G. Thompson, Alteration of the oceanic crust: processes and timing, Earth Planet, *Sci. Lett.* **52** (1978), pp. 311–327.

Ihinger et al., 1994 P.D. Ihinger, R.L. Hervig and P.F.M.J. McMillan, Analytical methods for volatiles in glasses. In: M.R. Carroll and J.R. Holloway, Editors, *Volatiles in Magmas, Rev. Mineral.* **vol. 30**, Mineral. Soc. of Am., Washington, DC (1994), pp. 67–112.

Imai et al., 1993 A. Imai, E.L. Listanco and T. Fujii, Petrologic and sulfur isotopic significance of highly oxidizing and sulfur-rich magma of Mt. Pinatubo, Philippines, *Geology* **21** (1993), pp. 699–702.

Imai et al., 1996 A. Imai, E.L. Listanco and T. Fujii, Highly oxidizing and sulfur-rich dacitic magma of Mount Pinatubo: implication for metallogenesis of porphyry copper mineralization in the Western Luzon Arc. In: Ch.G. Newhall and R.S. Punongbayan, Editors, *Fire and Mud. Eruptions and Lahars of Mount Pinatubo, Philippines*, University of Washington Press, Seattle (1996), pp. 865–874.

Ito et al., 1983 E. Ito, D.M. Harris and A.T. Anderson Jr., Alteration of oceanic crust and geologic cycling of chlorine and water, *Geochim. Cosmochim. Acta* **47** (1983), pp. 1613–1624.

Jégo et al., 2004 Jégo S., Polvé M., De Parseval Ph., Maury R. 2004. *Gold in Adakitic Magmas: Concentrations and Localisation within the Rocks.* Reunion de Sciences de la Terre RSTGV-A-00283 (pdf.).

Jochum and Verma, 1996 K.P. Jochum and S.P. Verma, Extreme enrichment of Sb, Tl and other trace elements in altered MORB, *Chem. Geol.* **130** (1996), pp. 289–299.

Keppler, 1996 H. Keppler, Constraints from partitioning experiments on the composition of subduction-zone fluids, *Nature* **380** (1996), pp. 237–240.

Keppler and Wyllie, 1991 H. Keppler and P.J. Wyllie, Partitioning of Cu, Sn, Mo, W, U, and Th between melt and aqueous fluid in the system haplogranite–H_2O–HCl and haplograbite–H_2O–HF, *Contrib. Mineral. Petrol.* **109** (1991), pp. 139–150.

Kogiso et al., 1997 T. Kogiso, Y. Tatsumi and S. Nakano, Trace element transport during dehydration processes in the subducted oceanic crust: 1. Experiments and implications for the origin of ocean island basalts, *Earth Planet. Sci. Lett.* **148** (1997), pp. 193–205.

Koepke and Behrens, 2001 J. Koepke and H. Behrens, Trace element diffusion in andesitic melts: an application of synchrotron X-ray fluorescence analysis, *Geochim. Cosmochim. Acta* **65** (2001), pp. 1481–1498.

London et al., 1988 D. London, R.L. Hervig and G.B. Morgan VI, Melt-vapor solubilities and elemental partitioning in peraluminous granite–pegmatite systems: experimental results with Macusani glass at 200 MPa, *Contrib. Mineral. Petrol.* **99** (1988), pp. 360–373.

Loucks and Mavrogenes, 1999 R.R. Loucks and J.A. Mavrogenes, Gold solubility in supercritical hydrothermal brines measured in synthetic fluid inclusions, *Science* **284** (1999), pp. 2159–2163.

Luhr and Melson, 1996 J.F. Luhr and W.G. Melson, Mineral and glass compositions in June 15, 1991, pumices: evidence for dynamic disequilibrium in the dacite of Mt. Pinatubo. In: Ch.G. Newhall and R.S. Punongbayan, Editors, *Fire and Mud. Eruptions and Lahars of Mt. Pinatubo, Philippines*, University of Washington Press, Seattle (1996), pp. 733–750.

Malihan, 1987 Malihan, T.D. 1987. *The Gold-rich Dizon porhyry Copper Mine in the Western Central Luzon Island, Philippines: Its Geology and Tectonic Setting: Proceedings of the Pacific Rim Congress'87, Australian Institutes of Mining and Metallurgy*. Parkville, Victoria, Australia, pp. 303–307.

McCulloch and Gamble, 1991 M.T. McCulloch and J.A. Gamble, Geochemical and geodynamical constraints on subduction zone magmatism, *Earth Planet. Sci. Lett.* **102** (1991), pp. 358–374.

Metrich and Rutherford, 1992 N. Metrich and M.J. Rutherford, Experimental study of chlorine behaviour in hydrous silicic melts, *Geochim. Cosmochim. Acta* **56** (1992), pp. 607–616.

Mungall, 2002 J.E. Mungall, Roasting the mantle: slab melting and the genesis of major Au and Au-rich Cu deposits, *Geology* **30** (2002), pp. 915–918.

Nesbitt et al., 1987 B.E. Nesbitt, R.M.St. Louis and K. Muehlenbachs, Distribution of gold in altered basalts of DSDP hole 504B, *Can. J. Earth Sci.* **24** (1987), pp. 201–209.

Noll et al., 1996 P.D. Noll Jr., H.E. Newsom, W.P. Leeman and J.G. Ryan, The role of hydrothermal fluids in the production of subduction zone magmas: Evidence from siderophile and chalcophile trace elements and boron, *Geochim. Cosmochim. Acta* **60** (1996), pp. 587–611.

Onishi and Sandell, 1955 H. Onishi and E.B. Sandell, Geochemistry of arsenic, *Geochim. Cosmochim. Acta* **7** (1955), pp. 1–33.

Pallister et al., 1996 J.S. Pallister, R.P. Hoblitt, G.P. Meeker, R.J. Knight and D.F. Siems, Magma mixing at Mount Pinatubo: petrographic and chemical evidence from the 1991 deposits. In: Ch.G. Newhall and R.S. Punongbayan, Editors, *Fire and Mud. Eruptions and Lahars of Mount Pinatubo, Philippines*, University of Washington Press, Seattle (1996), pp. 687–732.

Pasteris et al., 1996 J.D. Pasteris, B. Wopenka, A. Wang and T.N. Harris, Relative timing of fluid and anhydrite saturation: Another consideration in the sulfur budget of the Mount Pinatubo eruption. In: Ch.G. Newhall and R.S. Punongbayan, Editors, *Fire and Mud. Eruptions and Lahars of Mount Pinatubo, Philippines*, University of Washington Press, Seattle (1996), pp. 875–894.

Peacock et al., 1994 S.M. Peacock, T. Rushmer and A.B. Thompson, Partial melting of subducting oceanic crust, *Earth Planet. Sci. Lett.* **121** (1994), pp. 227–244.

Pearce et al., 1997 N.J.G. Pearce, W.T. Perkins, J.A. Westgate, M.P. Gorton, S.E. Jackson, C.R. Neal and S.P. Chenery, A compilations of new and published major and trace element data for NIST SRM 610 and NIST SRM 612 glass reference materials, *Geostand. Newslett.* **21** (1997), pp. 115–144.

Pichavant et al., 1987 Pichavant, M., Herrera, J.V., Boulmier, S., Briqueu, L., Joron, J-.L., Juteau, M., Marin, L., Michard, A., Sheppard, S.M., Treuil, M., Vernet, M., 1987. The macusani glasses, SE Peru: evidence of chemical fractionation in Peraluminous magmas. In: B.O. Mysen (eds.) *Magmatic Processes: Physicochemical Principles*, The Geochemical Society, Special Publications 1, pp. 359–373.

Pichavant et al., 1988 M. Pichavant, D.J. Kontak, L. Briqueu, J.V. Herrera and A.H. Clark, The miocene–pliocene Macusani Volcanics, SE Peru, *Contrib. Mineral. Petrol.* **100** (1988), pp. 325–338.

Pichler et al., 1991 T. Pichler, W.I. Ridley and E. Nelson, Low-temperature alteration of dredged volcanics from the Southern Chile Ridge: additional information about early stage of seafloor weathering, *Mar. Geol.* **159** (1991), pp. 155–177.

Plank and Langmuir, 1998 T. Plank and C.H. Langmuir, The chemical composition of subducting sediment and its consequences for the crust and mantle, *Chem. Geol.* **145** (1998), pp. 325–394.

Pokrovski et al., 2005 G.S. Pokrovski, J. Roux and J.-C. Harrichoury, Fluid density control on vapour-liquid partitioning of metals in hydrothermal systems, *Geology* **33** (2005), pp. 657–660.

Pokrovski et al., 2002 G.S. Pokrovski, I.V. Zakirov, J. Roux, D. Testemale, J.-L. Hazemann, A.Yu. Bychkov and G.V. Golikova, Experimental study of arsenic speciation in vapour phase to 500 °C: implications for As transport and fractionation in low-density crustal fluids and volcanic gases, *Geochim. Cosmochim. Acta* **66** (2002), pp. 3453–3480.

Polvé et al., 2004 Polvé, M., de Parseval, P., Jégo S., Maury, R.C. 2004. Where is the Gold in Adakites: Preliminary Results from a EMPA-SIMS Study, 57-OSE-A1547, Joint AOGS 1st Annual Meeting and second APHW Conference, Abstracts vol.1, 166.

Polvé et al., 2003 Polvé, M., Maury, R. Joron, J.L., 2003. *Slab Melting and the Origin of Gold in Au and Au–Cu Deposits: Geochemical Clues from Recent Adakites*. EGS meeting, Nice, Geophys. Res. Abstracts vol. 5, EGS-AGU-EUG Joint Assembly, EAE03-A-12068.

Prouteau et al., 1999 G. Prouteau, B. Scaillet, M. Pichavant and R.C. Maury, Fluid-present melting of ocean crust in subduction zones, *Geology* **27** (1999), pp. 1111–1114.

Prouteau and Scaillet, 2003 G. Prouteau and B. Scaillet, Experimental constraints on the origin of the 1991 Pinatubo dacite, *J. Petrol.* **44** (2003), pp. 2203–2241.

Qu et al., 2004 X. Qu, Z. Hou and Y. Li, Melt components derived from a subducted slab in late orogenic ore-bearing porhyries in the Gangdese copper belt, southern Tibetan plateau, *Lithos* **74** (2004), pp. 131–148.

Reich et al., 2003 M. Reich, M.A. Parada, C. Palacios, F. Schultz and B. Lehmann, Adakite-like signature of late Miocene intrusions at the Los Pelambres giant porhyry copper deposit in the Andes of Central Chile: metallogenic implications, *Miner. Dep.* **40** (2003), pp. 387–399.

Rutherford and Devine, 1996 M.J. Rutherford and J.D. Devine, Pre-eruption pressure–temperature conditions and volatiles in the 1991 dacitic magma of Mt. Pinatubo. In: Ch.G. Newhall and R.S. Punongbayan, Editors, *Fire and Mud. Eruptions and Lahars of Mt. Pinatubo, Philippines*, University of Washington Press, Seattle (1996), pp. 751–766.

Sajona and Maury, 1998 F.G. Sajona and R.C. Maury, Association of adakites with gold and copper mineralization in the Philippines, *C.R. Acad. Sci. IIA Earth Planet. Sci.* **326** (1998), pp. 27–34.

Scaillet et al., 1998 B. Scaillet, B. Clemente, B.W. Evans and M. Pichavant, Redox control of sulfur degassing in silicic magmas, *J. Geophys. Res.* **103** (1998) (B10), pp. 23937–23949.

Scaillet and Evans, 1999 B. Scaillet and B. Evans, The 15 June 1999 eruption of Mount Pinatubo. I Phase equilibria and pre-eruption P–T–f_{O2}–f_{H2O} conditions of the dacite magma, *J. Petrol.* **40** (1999), pp. 381–411.

Silver et al., 1990 L.A. Silver, P.D. Ihinger and E. Stolper, The influence of bulk composition on the speciation of water in silicate glasses, *Contrib. Mineral. Petrol.* **104** (1990), pp. 142–162.

Sen and Dunn, 1994 C. Sen and T. Dunn, Dehydration melting of a basaltic composition amphibolite at 1.5 and 2.0 Gpa: implications for the origin of adakites, *Contrib. Mineral. Petrol.* **117** (1994), pp. 394–409.

Sobolev and Chaussidon, 1996 A.V. Sobolev and M. Chaussidon, H_2O concentrations in primary melts from supra-subduction zones and mid-ocean ridges: implications for H_2O storage and recycling in the mantle, *Earth Planet. Sci. Lett.* **137** (1996), pp. 45–55.

Staudigel et al., 1981 H. Staudigel, S.R. Hart and S.H. Richardson, Alteration of the oceanic crust: process and timing, *Earth Planet. Sci. Lett.* **52** (1981), pp. 311–327.

Stolper and Newman, 1994 E. Stolper and S. Newman, The role of water in the petrogenesis of Mariana trough magmas, *Earth Planet. Sci. Lett.* **121** (1994), pp. 293–325.

Sun and McDonough, 1989 Sun, S-.S., McDonough, W.M. 1989. Chemical and isotope systematics of oceanic basalts: implications for mantle compositions and processes. In: Saunders, A.D., Norry, M.J. (eds.). *Magmatism in the Ocean Basins.* Geological Society Special London Publication 42, pp. 313–345.

Sun et al., 2004 W.D. Sun, R.J. Arculus, V.S. Kamenetsky and R.A. Binns, Release of gold-bearing fluids in convergent margin magmas prompted by magnetite crystallization, *Nature* **431** (2004), pp. 975–978.

Tatsumi and Kogiso, 1997 Y. Tatsumi and T. Kogiso, Trace element transport during dehydration processes in the subducted oceanic crust: 2. Origin of chemical and physical characteristics in arc magmatism, *Earth Planet. Sci. Lett.* **148** (1997), pp. 207–221.

Taylor et al., 1997 R.P. Taylor, S.E. Jackson, H.P. Longerich and J.D. Webster, In situ trace-element analysis of individual silicate melt inclusions by laser ablation microprobe-inductively coupled plasma-mass spectrometry-LAM-ICP-MS, *Geochim. Cosmochim. Acta* **61** (1997), pp. 2559–2567.

Thiéblemont et al., 1997 D. Thiéblemont, G. Stein and J.-L. Lescuyer, Gisements épithermaux et porphyriques: la connexion adakite. Epithermal and porphyry deposits: the adakite connection. C.R. Acad. Sci. Paris, Sciences de la terre et des planètes, *Earth Planet. Sci.* **325** (1997), pp. 103–109.

Urabe, 1985 T. Urabe, Aluminous granite as a source magma of hydrothermal ore deposits: an experimental study, *Econ. Geol.* **80** (1985), pp. 148–157.

Watson, 1994 E.B. Watson, Diffusion in volatile-bearing magmas. In: M.R. Carroll and J.R. Holloway, Editors, *Volatiles in Magmas, Rev. Mineral.* **vol. 30**, Mineral. Soc. of Am., Washington, DC (1994), pp. 67–121.

Webster, 1992a J.D. Webster, Fluid-melt interactions involving Cl-rich granites: experimental study from 2 to 8 kbar, *Geochim. Cosmochim. Acta* **56** (1992), pp. 659–678.

Webster, 1992b J.D. Webster, Water solubility and chlorine partitioning in Cl-rich granitic systems: effect of melt composition at 2 kbar and 800 °C, *Geochim. Cosmochim. Acta* **56** (1992), pp. 679–687.

Westrich and Gerlach, 1992 H.R. Westrich and T.M. Gerlach, Magmatic gas source for the stratosphere SO_2 cloud from the June 15, 1991, eruption of Mount Pinatubo, *Geology* **20** (1992), pp. 867–870.

Whalen et al., 2004 J.B. Whalen, V.J. McNicoll, A.G. Galley and F.J. Longstaffe, Tectonic and metallogenic importance of an Archean composite high- and low-Al tonalite suite, Western Superior Province, Canada, *Precambrian Res.* **132** (2004), pp. 275–301.

White et al., 1995 N.C. White, M.J. Leake, S.N. McCaughey and B.W. Parris, Epithermal gold deposits of the southwest Pacific, *J. Geochem. Explor.* **54** (1995), pp. 87–136.

Wiedenbeck et al., 2001 Wiedenbeck, M., Rocholl, A., Koepke, J. 2001. *Water—A Source of Systematic Error in Quantitative SIMS Analyses of Hydrous Glasses.* 11th Annual V.M. Goldschmidt Conference, Hot Spring, Virginia, USA, 3604.

Wood and Samson, 1998 Wood, S.A., Samson, I.M., 1998. Solubility of ore minerals and complexation of ore metals in hydrothermal solutions. In: Richrards, J.P., Larson, P.B. (Eds.), *Techniques in Hydrothermal Ore Deposits Geology.* Review in Economic Geology 10, Society of Economic Geologists, inc. p. 255.